Summary of Research

Prepared under NASA Grant NAG-1-1821

NASA Langley Research Center
Hampton, VA 23681-0001

Aerodynamic Modeling for Aircraft in Unsteady Flight Conditions

for the period of

March 22, 1996 to September 30, 1999

C. Edward Lan
Principal Investigator

April 6, 2000

The Flight Research Laboratory
The University of Kansas Center for Research, Inc.
2291 Irving Hill Road
Lawrence, Kansas 66045-2969

This report summarizes the activities in unsteady aerodynamic modeling and application of unsteady aerodynamic models to flight dynamics. A public briefing was presented on July 21, 1999 at Langley Research Center. A copy of that briefing is attached.

1. Unsteady Aerodynamic Modeling

1.1 Fourier Functional Analysis

The Fourier functional analysis to generate aerodynamic indicial integrals was developed in Ref. 1. The computer code to calculate the model coefficients was further improved in Ref. 2. However, the code still requires a user's occasional intervention to obtain reasonable results. To make the code more user-independent, the following improvements have been made:

(1) The best values of the initial input variables for C_L-, C_D- and C_m-models are now chosen internally in the code.

(2) A systematic mechanism is established to allow a user to restart the calculation for a better solution.

The resulting code has been applied to the F-18 and F-16XL data in the analysis of random gust response. As a result, a paper in random gust response was written and has been accepted for publication in the AIAA Journal (Ref. 3).

1.2 Generalized Dynamic Aerodynamic Models

The aerodynamic model based on indicial integrals is valid to represent the aerodynamics in unsteady flight conditions. However, this model may require too much computing time for real time simulation and does not clearly reveal the flight conditions for dynamic instability. As an alternative, a generalized dynamic aerodynamic coefficient model, which is frequency- and amplitude-dependent, is proposed. The results were published in Ref. 4.

In addition, the developed models were also applied to the prediction of aircraft-pilot coupling (Ref. 5).

1.3 Fuzzy Logic Modeling

The modeling methods described in Sections 1.1 and 1.2 are applicable when only one motion variable, such as the angle of attack, appears in the model. To generalize the aerodynamic modeling methods to more motion variables, we developed a fuzzy logic modeling algorithm that could handle complex modeling problems, such as one involving the angle of attack, sideslip, control deflections, etc. Using this method, we developed a longitudinal unsteady aerodynamic model for an F-16XL configuration by combining more than 200 different data sets into one model. The results were published in Ref. 6.

The same modeling technique was also applied to the rolling and yawing oscillation data for the F-16XL configuration. It was also possible to incorporate the rotary balance data into the present model. The rotary balance data are regarded as steady flow data and had to be represented as a separate aerodynamic model in the past. The results were published in Ref. 7.

2. Flight Dynamic Simulation

The established unsteady Aerodynamic models for the F-16XL have been successfully incorporated into a conventional flight simulation code for the purpose of investigating the unsteady aerodynamic effects on flight dynamics. The ultimate purpose is to determine whether using the unsteady aerodynamics models is more realistic in design for flight safety and in pilot training in flight simulators. The results will be presented in August 2000 (Ref. 8).

3. References

(1) Chin, S., and Lan, C. E., "Fourier Functional Analysis for Unsteady Aerodynamic Modeling," *AIAA Journal*, Vol. 30, September 1992, pp.2259-2266.

(2) Hu,C. C.; Lan, C. E. and Brandon, J., "Unsteady Aerodynamic Models for Maneuvering Aircraft," AIAA Paper 93-3626-CP, Aug. 1993.

(3) Lee, Y. N. and Lan, C. E., "Analysis of Random Gust Response with Nonlinear Unsteady Aerodynamics," accepted for publication in the *AIAA Journal*, May 2000.

(4) Lin, G. F.; Lan, C. E. and Brandon, J. M., "A Generalized Dynamic Aerodynamic Coefficient Model for Flight Dynamic Applications," AIAA Paper 97-3643, Aug. 1997.

(5) Lin, G. F.; Lan, C. E. and Brandon, J. M., "Simulation of Aircraft-Pilot Coupling as Limit-Cycle Oscillations," AIAA Paper 98-4147, Aug. 1998.

(6) Wang, Z.; Lan, C. E. and Brandon, J. M., "Fuzzy Logic Modeling of Nonlinear Unsteady Aerodynamics," AIAA Paper 98-4351, Aug. 1998.

(7) Wang, Z.; Lan, C. E. and Brandon, J. M., "Fuzzy Logic Modeling of Lateral-Directional Unsteady Aerodynamics," AIAA Paper 99-4012, Aug. 1999.

(8) Wang, Z.; Lan, C. E. and Brandon, J. M., "Unsteady Aerodynamic Effects on the Flight Characteristics of an F-16XL Configuration," AIAA Paper 2000-3910, to be published and presented in Aug. 2000.

Unsteady Aerodynamic Modeling and Applications

C. Edward Lan
Department of Aerospace Engineering
The University of Kansas
Lawrence, Kansas 66045

July 21, 1999

NASA Langley Research Center
Hampton, Virginia

Outline of Presentation

⇒ Motivation and Objectives

⇒ Unsteady Aerodynamic Phenomena

⇒ Overview of Unsteady Aerodynamics Modeling Techniques

⇒ Fuzzy Logic Modeling

⇒ Example Unsteady Aerodynamics Models

⇒ Applications of Unsteady Aerodynamic Models

⇒ Recommendations

Motivation and Objectives

• Motivation: Aerodynamic environment is unsteady in nature. However, aircraft are mostly designed for steady flow conditions. There may be uncertainties in performance, stability and control within the flight envelope.

• Objectives: The goal of unsteady aerodynamic modeling is to develop aerodynamic models which are applicable to steady and unsteady flow conditions for the analysis of performance, stability and control of air vehicles.

Unsteady Aerodynamic Phenomena

- Production of lift, drag and thrust is frequently not steady.

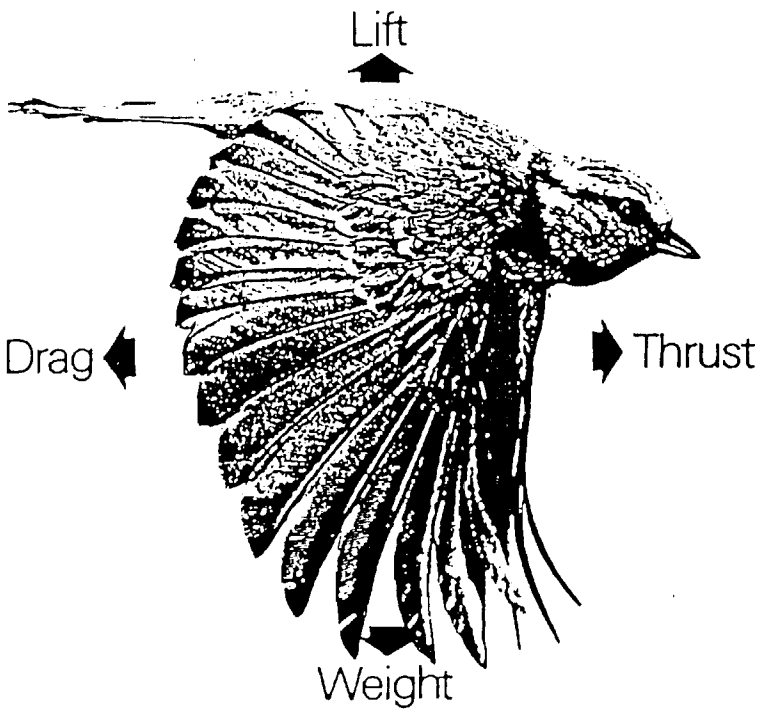

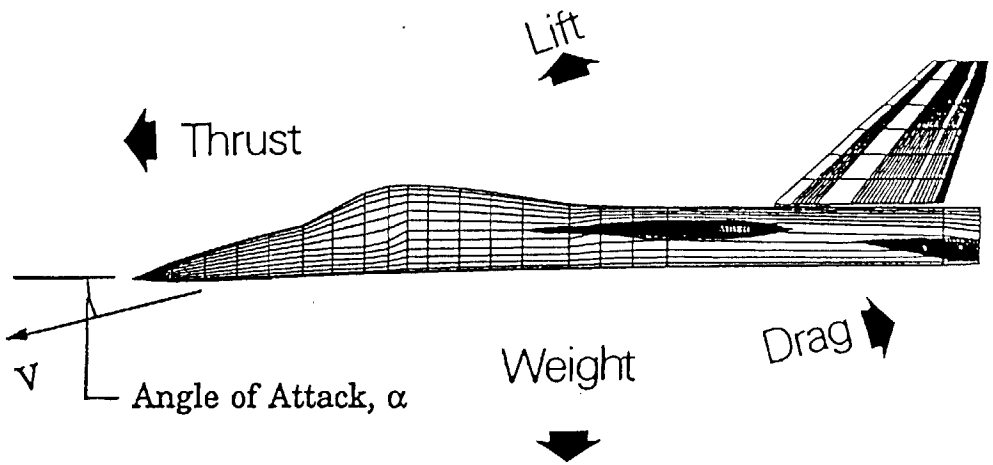

- Classical unsteady effects - circulatory flow

  · Aerodynamic lag in response caused by shed vortices (Wagner effect)

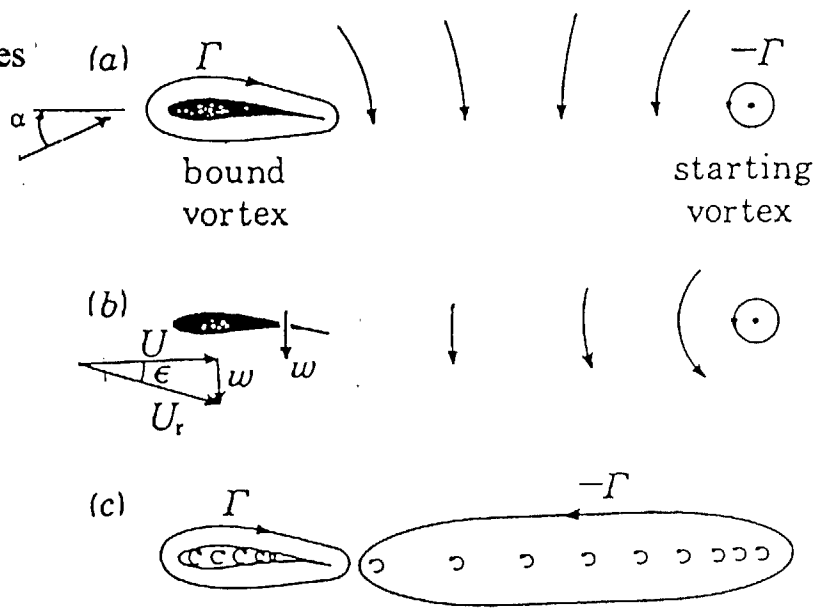

  · Aerodynamic lag in response caused by a finite propagation speed of disturbances (High speed applications)

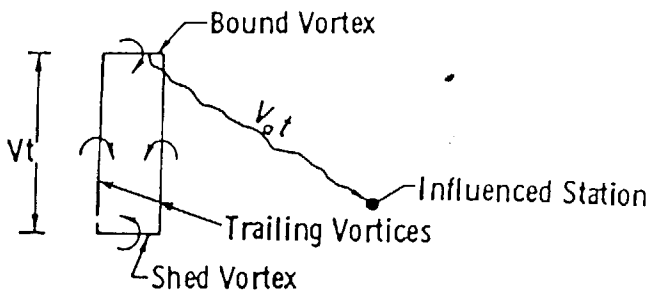

  · Classical aerodynamic lag does not provide sufficient explanation to natural flight phenomena.

- Dynamic stall: when the angle of attack is increased dynamically, vortices are created to change the aerodynamics:

  · Viscous boundary layer separates and a discrete vortex is generated.

  · Vortex detaches and moves downstream over the airfoil surface.

  · Vortex produces higher suction pressure on the upper surface.

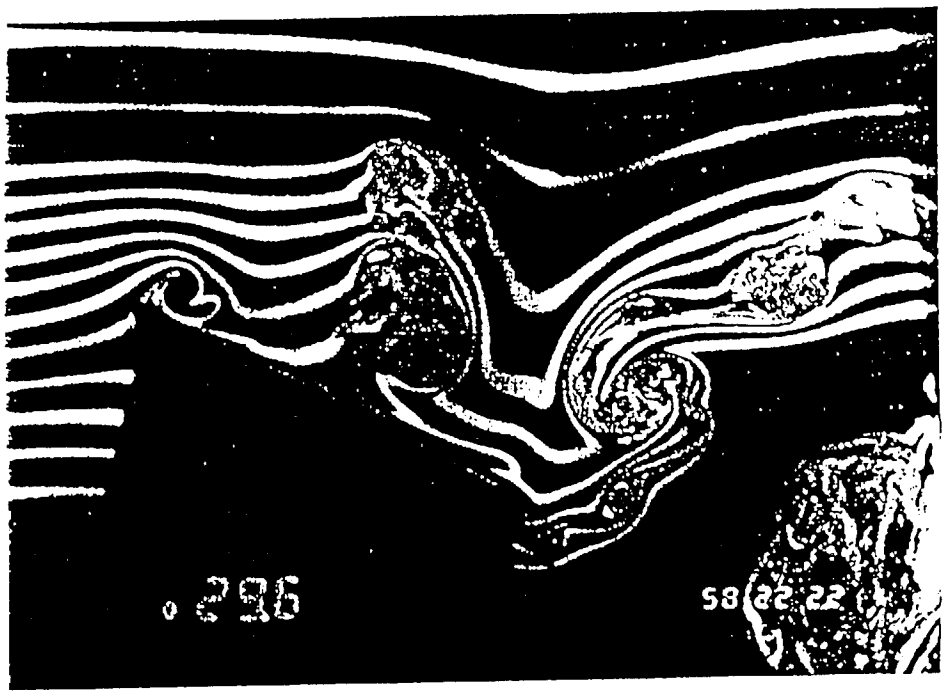

Air & Space, Oct./Nov. 1986

·Aerodynamic forces and moments depend strongly on the location of vortex and are therefore a function of time.

- Edge-separated vortices:

  · On a low aspect-ratio wing, if an edge-separated vortex flow is present, this vortex flow will not achieve its steady-state position and strength instantaneously in unsteady motion, thus creating vortex lag.

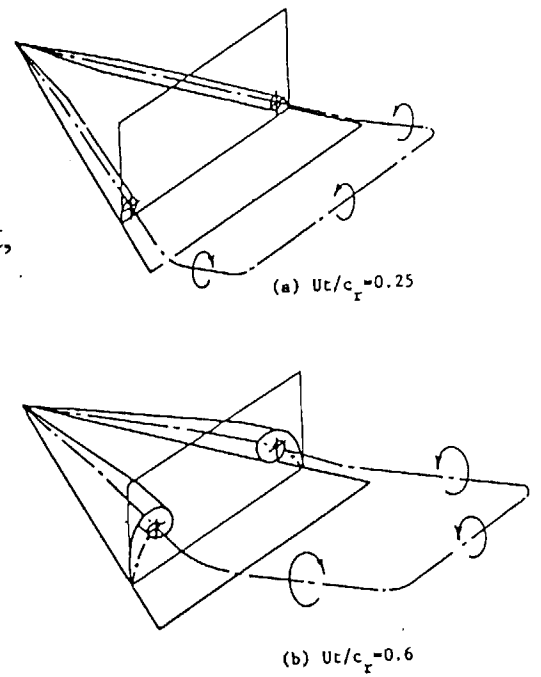

Lambourne, et al. British ARC R & M 3645, 1969

  · If vortex breakdown cannot be avoided, the breakdown phenomena will lag behind the motion, thus increasing the lift if the angle of attack is increasing.

- Interaction among various mechanisms.

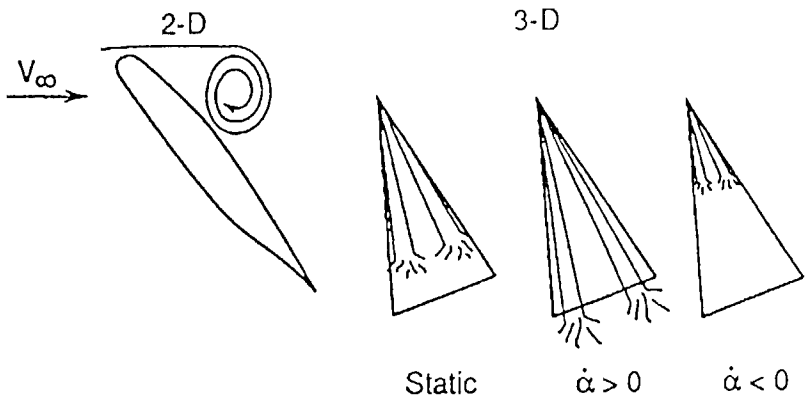

Brandon, AGARD R-776, 1991

Overview of Unsteady Aerodynamics Modeling Techniques

- Existing Available Methods:
  - · Quasi-steady aerodynamics in tabulated form.
  - · State-space representation
  - · Nonlinear indicial function model
  - · Nonlinear indicial integrals through Fourier functional analysis
  - · Generalized dynamic aerodynamic coefficient model
- Most existing unsteady aerodynamic modeling methods have dealt with only one motion variable: the angle of attack

• Quasi-Steady Aerodynamics

· Unsteady aerodynamic effect is represented through dynamic stability parameters which are obtained in small-amplitude forced oscillation tests at a pre-determined frequency at a given angle of attack.

·The representation of unsteady aerodynamics by a linear decomposition into the in-phase and out-of-phase responses is inadequate at high alphas.

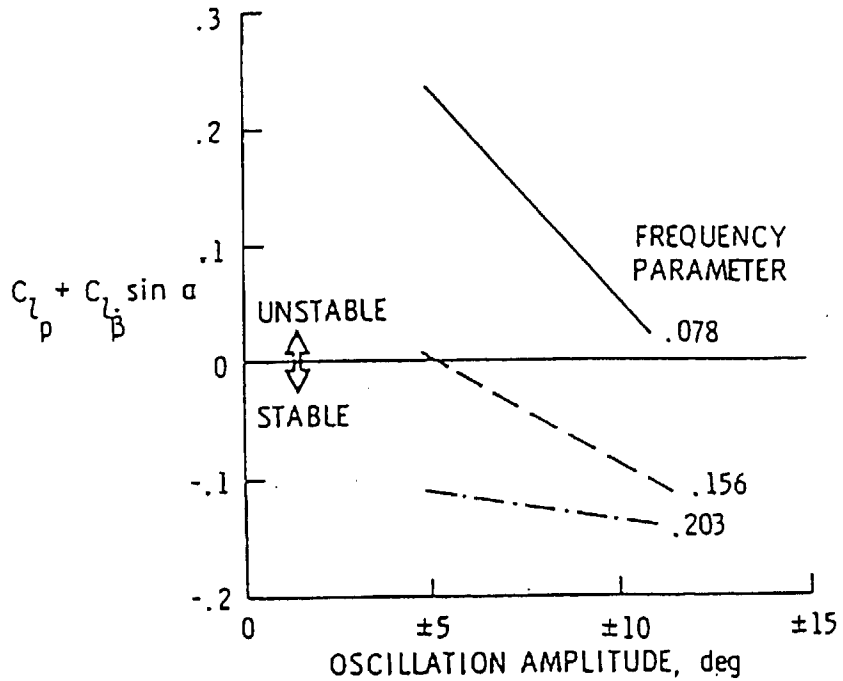

• State-Space Representation

References:
(1) M. Goman and A. Khrabrov, "State-Space Representation of Aerodynamic Characteristics of an Aircraft at High Angles of Attack," *Journal of Aircraft*, Vol. 31, No. 5, 1994, pp. 1109-1115.
(2) Y. Fan and F. H. Lutze, "Identification of an Unsteady Aerodynamic Model at High Angles of Attack," AIAA Paper 96-3407, July 1996.

· Input-state-output dynamical system:

$$dx/dt = f(x,h) \qquad C = g(x,h)$$

where x is the flow state variable,
h = system inputs
C = aerodynamic force and moment coefficients

· Fluid mechanics processes that have been modeled:
  · quasi-steady aerodynamic effects, such as aerodynamic lag, boundary-layer improvements, etc.
  · transient aerodynamic effects, such as the relaxation process in separated flow adjustment.

· Fluid mechanics processes that have been excluded:
  · Effects of "spilled vortex" and "wake vortex sheet".
  · Virtual mass effect.
  · Multiple vortices and synergistic effects.

• Nonlinear Indicial Function Model

References: (1) P. H. Reisenthel, "Development of a Nonlinear Indicial Model for Maneuvering Fighter Aircraft," AIAA Paper 96-0896, Jan. 1996.

(2) P. H. Reisenthel, "Application of Nonlinear Indicial Modeling to the Prediction of Dynamically Stalling Wing," AIAA Paper 96-2493, July 1996.

· Model

· Without flow bifurcation:

The generalized Duhamel convolution integral is assumed valid:

$$C_L = C_L(0) + \int_0^t \left[\frac{\delta C_L(t-\tau)}{\delta\alpha}\right]_\tau \frac{d\alpha}{d\tau} d\tau$$

where

$$\frac{\delta C_L(\alpha(\xi);t,\tau)}{\delta\alpha} = \lim_{\Delta\alpha\to 0}\left[\frac{C_L(\alpha(\xi)+H(\xi-\tau)\Delta\alpha)-C_L(\alpha(\xi))}{\Delta\alpha}\right]$$

where H is the Heaviside step function. $(\delta C_L/\delta\alpha)_\tau$ is called the indicial response.

· In applications, the generated indicial functions are defined as functions of α and $\dot{\alpha}$ and interpolation is made to choose a particular indicial function to be used.

- **Nonlinear Indicial Integrals through Fourier Functional Analysis**

  Refs. AIAA Journal Sept. 1992, p.2259

  AIAA Paper 93-3626

- Test data from large-amplitude forced oscillation testing in pitch with several oscillation frequencies are analyzed through Fourier Functional Analysis.

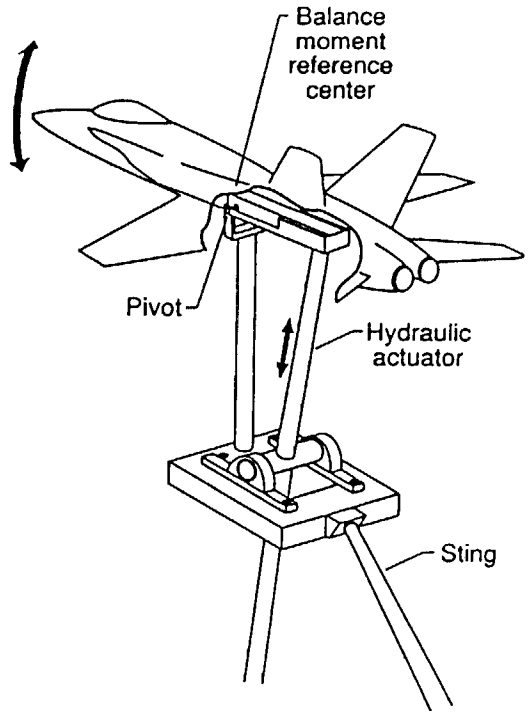

- The results are recast in the form of:

$$C_m = A_o(k) + \sum_{j-1}^{m} C_j(E_{1j}\dot{\alpha}_j + E_{2j}\ddot{\alpha}_j) + \sum_{j-1}^{m} C_j(\textit{amplitude function})_j(\textit{phase function})_j$$

$$-A_o(k) + \sum_{j-1}^{m} C_j(E_{1j}\dot{\alpha}_j + E_{2j}\ddot{\alpha}_j) + C_1(H_{11}\alpha + H_{21}\dot{\alpha})(1.-PD_1)$$

$$+ C_2(H_{12}\alpha^2+H_{22}\alpha\dot{\alpha}+H_{32}\dot{\alpha}^2)(1.-PD_2) + C_3(H_{13}\alpha^3+H_{23}\alpha^2\dot{\alpha}+H_{33}\alpha\dot{\alpha}^2+H_{43}\dot{\alpha}^3)(1.-PD_3)$$

$$+ \ldots$$

where PD's are Padé approximants of order 2 and are defined as:

$$PD_j = \frac{P_{1j}(ik)^2 + P_{2j}(ik)}{P_{3j}(ik)^2 + ik + P_{4j}}$$

• By Fourier inversion, longitudinal aerodynamics are finally represented in the form of indicial integrals:

$$C_m(t') = C_{m_{indicial}}[t' - \tau,\ \alpha(\tau),\ \dot{\alpha}(\tau)]_{\tau=0} + C_{ave} + \sum_{j=1}^{m} C_j * (E_{1j}\dot{\alpha}_j + E_{2j}\ddot{\alpha}_j)$$
$$+ \sum_{j=1}^{m} C_j \int_0^{t'} \frac{d(a.f.)_j}{d\alpha}(1. - a_{1j}e^{-a_{3j}\, j\, (t'-\tau)} - a_{2j}e^{-a_{4j}\, j\, (t'-\tau)})\frac{d\alpha(\tau)}{d\tau}d\tau$$
$$+ \frac{l}{V_\infty}\sum_{j=1}^{m} C_j \int_0^{t'} \frac{d(a.f.)_j}{d\dot{\alpha}}(1. - a_{1j}e^{-a_{3j}\, j\, (t'-\tau)} - a_{2j}e^{-a_{4j}\, j\, (t'-\tau)})\frac{d\dot{\alpha}(\tau)}{d\tau}d\tau$$

• For an arbitrary motion, the angle of attack $\alpha_1(\tau)$ and $\dot{\alpha}_1$ at a given time can be expressed by an equivalent harmonic motion, which has the same mean α_M and amplitude α_A of the oscillation experiments:

$$\alpha_1(\tau) = \alpha_M + \alpha_A \cos(k_{eff}\tau + \phi_{eff})$$

$$\dot{\alpha}_1(\tau) = -\alpha_A k_{eff} \sin(k_{eff}\tau + \phi_{eff})$$

- The effective frequency can be obtained analytically:

$$k_{eff} = \frac{\pm \dot{\alpha}_1}{\sqrt{\alpha_A^2 - (\alpha_1 - \alpha_M)^2}}$$

- To compare with the conventional small-amplitude forced-oscillation testing:

  · In wind-tunnel testing, Δq is the same as $\Delta\dot{\alpha}$:

$$\Delta\alpha = \alpha_a \cos\theta, \quad \Delta\dot{\alpha} = -\alpha_a k \sin\theta$$

$$\Delta q = -\alpha_a k \sin\theta, \quad \Delta\dot{q} = -\alpha_a k^2 \cos\theta$$

Damping and stiffness derivatives:

$$C_{m_q} + C_{m_\alpha} = -\frac{1}{\pi k \alpha_a} \int_0^{2\pi} C_m \sin\theta \, d\theta$$

$$C_{m_\alpha} - k^2 C_{m_{\dot{q}}} = -\frac{1}{\pi \alpha_a} \int_0^{2\pi} C_m \cos\theta \, d\theta$$

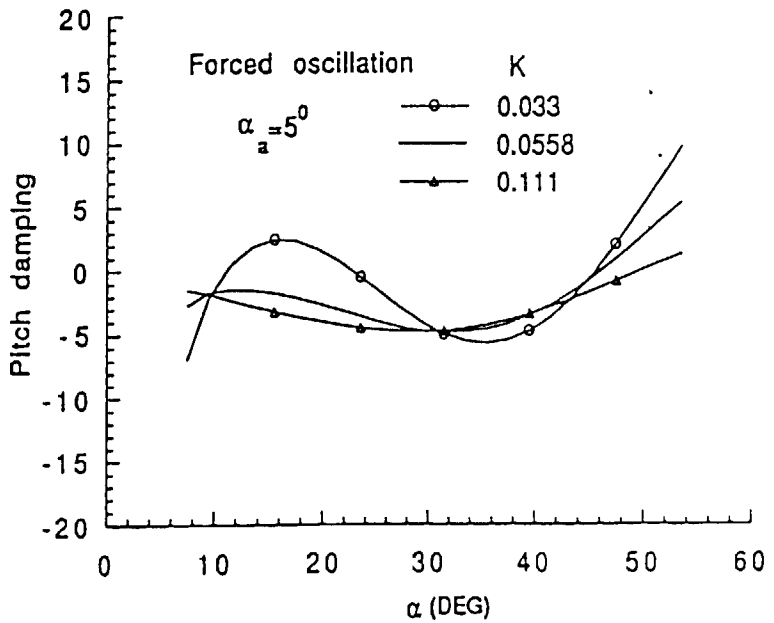

- Typical lift and moment data for an F-18 configuration: 5 Fourier terms

  - A clockwise loop in C_m implies negative pitch damping.

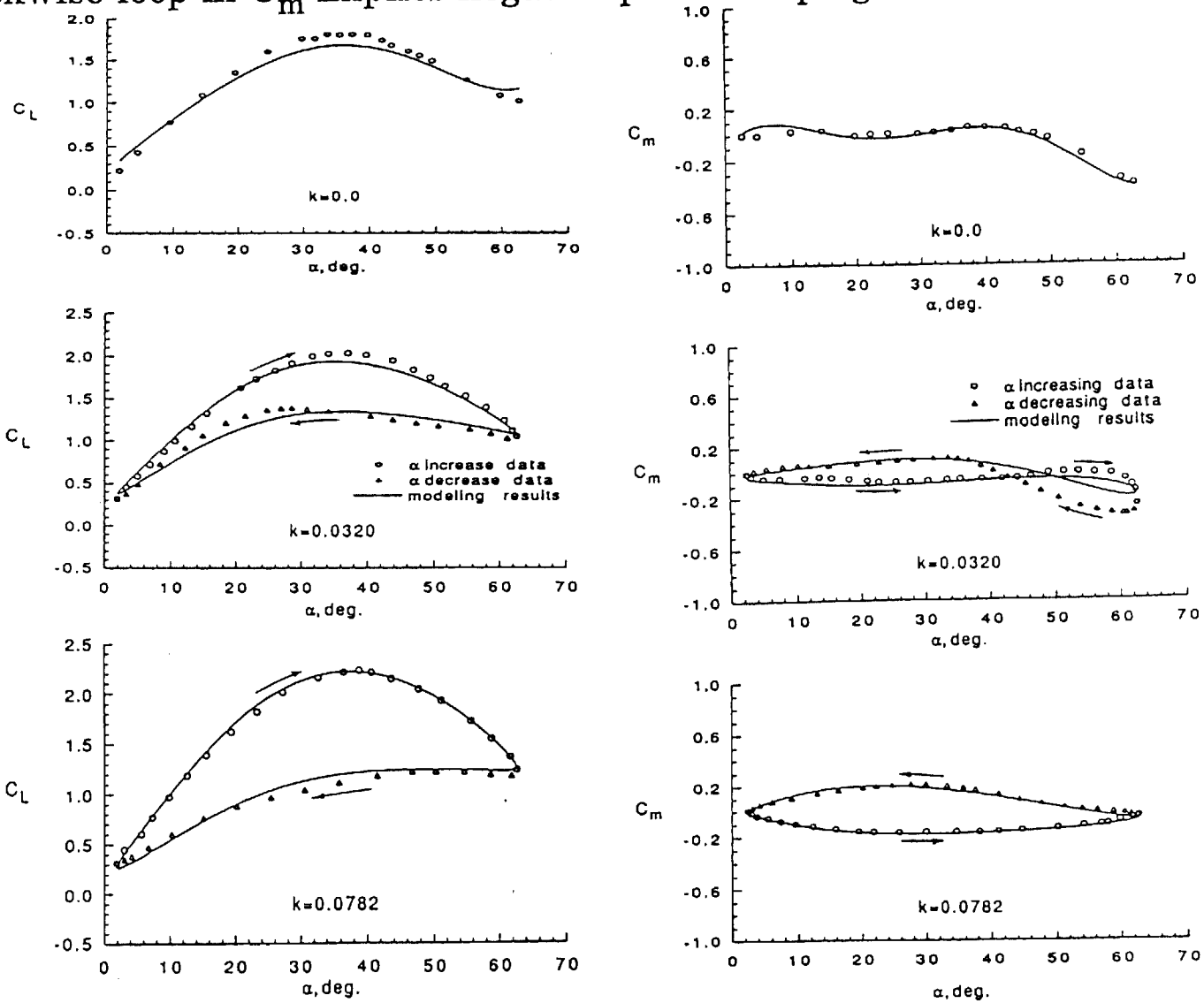

- **Generalized Dynamic Aerodynamic Coefficient Model**

  - The aerodynamic coefficient is assumed to be of the form:

$$C_a = C_o + C_1\alpha + C_2\alpha^2 + C_3\alpha|\alpha| + C_4\alpha^3 + C_5\dot{\alpha} + C_6\alpha\dot{\alpha} + C_7|\alpha|\dot{\alpha} + C_8|\dot{\alpha}|\dot{\alpha}$$

  · C_a = the aerodynamic coefficients, such as C_L, C_D and C_m in pitching motion.
  ·The data base for modeling: forced oscillation tests at several frequencies, including static testing.
  · The coefficients C_i's are all functions of the reduced frequency.
  · C_i's have similar significance in stability analysis to the stability parameters in the conventional method.
  · It can model the nonlinear motion phenomena, such as pitch limit-cycle oscillation, and wing rock if α is replaced with the roll angle ϕ.

- A general motion is described by an equivalent harmonic motion at a given time

F-18 HARV configuration

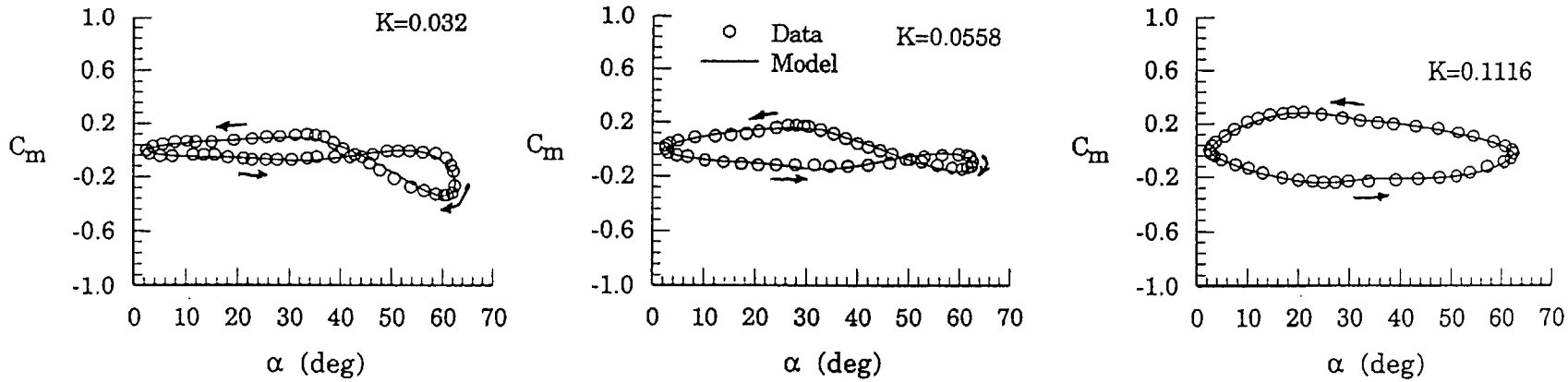

FUZZY LOGIC

· Consider a collection of 10 people, x_1, x_2, ..., x_{10}, forming a project team. The entire object is called the Universe of Discourse:

$$X = \{ x_1, x_2, ..., x_{10} \}$$

The set of males in X is

$$A = \{ x_1, ..., x_4 \}$$

This is expressed by the mapping μ_A from X into the binary space {0,1}:

$$\mu_A: X \rightarrow \{0, 1\}$$
$$\mu_A (x) = 0, \quad x = x_5, ..., x_{10}$$
$$1, \quad x = x_1, ..., x_4$$

Crisp Set: Only 0 or 1 is possible.

· However, the concept of "young male" or "beautiful female" would be difficult to define with a crisp set.

Fuzzy Set: Allows a degree of belonging, such as 0.5 or 0.8.

Example: Patients suffering from hepatitis show in 60% of all cases **high fever**, in 45% of all cases a **yellowish colored skin**, and 30% of all cases **nausea**.
High fever, yellowish colored skin and nausea are all "fuzzy".

Example: FAA wake vortex separation standards:

	Leading aircraft		
Following aircraft	heavy	large	small
heavy	4	3	3
large	5	3	3
small	6	4	3

heavy aircraft: $W \geq 300{,}000$ lbs
large aircraft: $12{,}500 < W < 300{,}000$ lbs
Small aircraft: $W < 12{,}500$ lbs

· Question: How about aircraft with $W = 295{,}000$ lbs ?

Probability theory:
Models stochastic uncertainty of whether a certain event will take place

Fuzzy Logic:
Models the uncertainty of the definition of the event itself

Fuzzy Logic Modeling

• All Existing Unsteady Aerodynamics Modeling Techniques: Difficulty in generalization to multiple motion variables and control surface deflections.

• Advantage of Fuzzy Logic Algorithm: Multi-dimensional, nonlinear interpolation scheme
  · No functional form between the input and output variables is needed.
  · Complex motions involving several variables can be handled.

• Overview

·Each motion variable is divided into a number of ranges in values (called membership functions)

·Each combination of membership functions, one from each motion variable, constitutes a fuzzy cell.

· Each fuzzy cell contributes to the prediction of the value of an aerodynamic coefficient equal to P^i (internal functions) with an associated weighting factor.

· The final prediction of an aerodynamic coefficient is equal to the weighted average of contributions of all fuzzy cells.

· Internal functions

Internal functions are assumed to be linear functions of input parameters as follows

$$P^i = y_i(x_1, x_2, \cdots, x_r, \cdots, x_k) =$$
$$p_0^i + p_1^i x_1 + \cdots + p_r^i x_r + \cdots + p_k^i x_k$$

p_r^i = the unknown coefficients to be determined,
y_i represents the aerodynamic force or moment coefficients
x_r the motion variables, such as α, $\dot{\phi}$, $\dot{\psi}$, etc.

· Membership functions and fuzzy rules

· The values of each fuzzy variable are divided into membership functions.

· The membership grading also ranges from 0 to 1.0, with "0" meaning no effect, and "1" meaning a full effect.

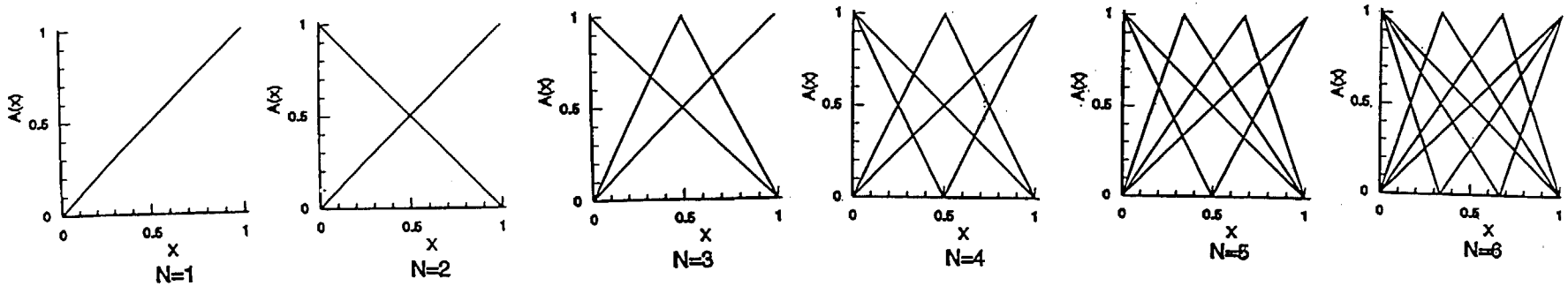

· A fuzzy cell is formed by taking one membership function from each variable. The rule of the i-th cell is stated as:

if x_1 *is* $A_1^i(x_1)$, *and if* x_2 *is* $A_2^i(x_2)$, *and ... and if* x_k *is* $A_k^i(x_k)$,
then the cell output is $P^i = p_0^i + p_1^i x_1 + p_2^i x_2 + \ldots + p_k^i x_k$

where $A_k^i(x_k)$ denotes the membership function for x_k. Corresponding to each cell, there is one internal function to calculate the cell's output.

· Output

· The output of the fuzzy logic model is the weighted average of all the cell outputs.

· The weight of each cell's output is taken to be the product operation of all the membership grades, represented by product$[A_1^i(x_1), A_2^i(x_2), \cdots, A_r^i(x_r), \cdots, A_k^i(x_k)]$

· The output estimated by the fuzzy logic model corresponding to the input $(x_1, x_2, \cdots, x_k)$ is

$$\hat{y} = \frac{\sum_{i=1}^{n} \text{product}[A_1^i(x_1), \cdots, A_r^i(x_r), \cdots, A_k^i(x_k)] P^i}{\sum_{i=1}^{n} \text{product}[A_1^i(x_1), \cdots, A_r^i(x_r), \cdots, A_k^i(x_k)]}$$

· n is the total number of cells of the model.

· Parameter Identification

· The unknown coefficients of the internal functions are determined with the Newton gradient-descent method.

· The accuracy of the established fuzzy logic model is described by the summation of squared errors (SSE) and the multiple correlation coefficient, R^2, defined as

$$SSE = \sum_{j=1}^{m} (\hat{y}_j - y_j)^2$$

$$R^2 = 1 - \frac{\sum_{j=1}^{m} (\hat{y}_j - y_j)^2}{\sum_{j=1}^{m} (\bar{y} - y_j)^2}$$

$\hat{y}_j$ = the output of the fuzzy logic model,

y_j = the data point used for the model training, and $\bar{y}$ = is the mean of the sample data.

· Conceptually, this is similar to the stepwise regression method in flight data analysis.

· The parameters associated with the internal functions are identified with Newton's method to minimize SSE:

· for r = 0,

$$p^{i}_{0,\,t+1} = p^{i}_{0,\,t} - 2\alpha_0(\hat{y}_j - y_j) \times \frac{\text{product}[A_1^i(x_{1,j}),\cdots,A_r^i(x_{r,j}),\cdots,A_k^i(x_{k,j})]}{\sum_{s=1}^{n}\text{product}[A_1^s(x_{1,j}),\cdots,A_r^s(x_{r,j}),\cdots,A_k^s(x_{k,j})]}$$

· for r = 1, 2, ···, k,

$$p^{i}_{r,\,t+1} = p^{i}_{r,\,t} - 2\alpha_r(\hat{y}_j - y_j) \times \frac{\text{product}[A_1^i(x_{1,j}),\cdots,A_r^i(x_{r,j}),\cdots,A_k^i(x_{k,j})]x_{r,j}}{\sum_{s=1}^{n}\text{product}[A_1^s(x_{1,j}),\cdots,A_r^s(x_{r,j}),\cdots,A_k^s(x_{k,j})]}$$

· The number of membership functions ($g_1, g_2, \ldots g_r, \ldots g_k$) is determined by having the largest value of multiple correlation coefficient R^2.

- Three codes have been developed for fuzzy logic modeling:

  · "struc.f" - to identify the structure of the membership functions. Users must customize the code by specifying the input variables and the value ranges of these variables.

  ⇒ Input file to be prepared by the user (title not included):

t	α	$\dot{\alpha}$	$\ddot{\alpha}$	k	β	δ_e	C_L
0.000	0.000	0.000	243.935	0.1124	-5.000	0.000	0.075800
0.040	0.192	9.668	242.596	0.1124	-5.000	0.000	0.076700
0.090	0.972	21.627	237.159	0.1124	-5.000	0.000	0.106100
0.140	2.347	33.264	227.580	0.1124	-5.000	0.000	0.160400
0.190	4.289	44.318	214.045	0.1124	-5.000	0.000	0.246200
0.241	6.825	54.817	196.370	0.1124	-5.000	0.000	0.364900
0.292	9.919	64.446	174.806	0.1124	-5.000	0.000	0.512300
0.340	13.142	72.164	152.344	0.1124	-5.000	0.000	0.686000
0.390	16.973	79.201	125.642	0.1124	-5.000	0.000	0.874600
0.440	21.037	84.728	97.317	0.1124	-5.000	0.000	1.034200
0.492	25.639	89.034	65.240	0.1124	-5.000	0.000	1.240500
0.539	29.890	91.410	35.617	0.1124	-5.000	0.000	1.404900
0.590	34.491	92.390	3.549	0.1124	-5.000	0.000	1.512400
0.640	39.102	91.763	-28.589	0.1124	-5.000	0.000	1.565100
0.689	43.640	89.540	-60.220	0.1124	-5.000	0.000	1.533000
0.739	48.030	85.758	-90.813	0.1124	-5.000	0.000	1.457700
0.789	52.192	80.485	-119.818	0.1124	-5.000	0.000	1.325200
0.840	56.109	73.704	-147.118	0.1124	-5.000	0.000	1.201400
0.890	59.552	65.852	-171.117	0.1124	-5.000	0.000	1.046900

  ⇒ Another input file - "parent.inp" is needed for restart purpose.

  · "model.f" - to refine the results from "struc.f". No additional input is needed.

  · "predict.f" - to predict the results. It requires one input file: predict.inp using the same format as for "struc.f".

Example Unsteady Aerodynamics Models

· F16XL Longitudinal Aerodynamics

The unsteady aerodynamic coefficients are assumed to be functions of angle of attack α, rate of angle of attack $\dot{\alpha}$, $\ddot{\alpha}$, the reduced frequency of the forced oscillation testing, k, and sideslip angle β, and elevator deflection angle δ_e; that is,

$$C_{L,D,m,y,n,l} = f(\alpha, \dot{\alpha}, \ddot{\alpha}, k, \beta, \delta_e)$$

· The ranges of the motion variables are defined as:

$\alpha_{min} = -10°$, $\alpha_{max} = 80°$

$\dot{\alpha}_{min} = -250°/s$, $\dot{\alpha}_{max} = 250°/s$

$\ddot{\alpha}_{min} = -2800°/s^2$, $\ddot{\alpha}_{max} = 2800°/s^2$

$k_{min} = 0.0$, $k_{max} = 0.8$

$\beta_{min} = -30°$, $\beta_{max} = 0.0°$, $\delta_{emin} = -25°$, $\delta_{emax} = 25°$

· All input variables are normalized to the domain of [0, 1]:

$$\alpha_{new} = \frac{\alpha - \alpha_{min}}{\alpha_{max} - \alpha_{min}}$$

· The model structure was determined to be:

Coefficient	α $\dot{\alpha}$ $\ddot{\alpha}$ k β δ_e	number of rules
C_L	4 x 3 x 4 x 3 x 3 x 2	864
C_D	3 x 3 x 2 x 3 x 2 x 2	216
C_m	5 x 4 x 2 x 3 x 3 x 4	1440
C_y	6 x 3 x 2 x 2 x 3 x 2	432
C_n	4 x 4 x 2 x 2 x 3 x 2	384
C_ℓ	5 x 3 x 2 x 2 x 4 x 2	480

· For example, lift coefficient model with the structure: (4,3,4,3,3,2) means that the numbers of membership functions for the lift coefficient are 4 for α, 3 for $\dot{\alpha}$, 4 for $\ddot{\alpha}$, 3 for k, 3 for β and 2 for δ_e.

· **A numerical example**: Assume the input variables to the model are:

$$\alpha = 7.8°, \quad \dot{\alpha} = 11.53°/s, \quad \ddot{\alpha} = 7.457°/s^2, \quad k = 0.0223, \quad \beta = 0., \quad \delta_e = 0.$$

· When these are substituted into the following equation,

$$\hat{y} = \frac{\sum_{i=1}^{n} \text{product}[A_1^i(x_1),\cdots,A_r^i(x_r),\cdots,A_k^i(x_k)]P^i}{\sum_{i=1}^{n} \text{product}[A_1^i(x_1),\cdots,A_r^i(x_r),\cdots,A_k^i(x_k)]}$$

the following results can be obtained for the membership functions:
$A_1(1) = .1977777$, $A_2(1) = .5230659$, $A_3(2) = .4986683$
$A_4(3) = 5.57500E\text{-}02$, $A_5(1) = 1.0$, $A_6(2) = .5$

The coefficients for the internal function (1,1,2,3,1,2) are
$p_0 = 2.01212$, $p_1 = -5.0711$, $p_2 = -1.56532$, $p_3 = 3.2326$, $p_4 = 1.45039$
$p_5 = 2.135$, $p_6 = .27386$

The values of fuzzy variables are, after converted to [0,1]:
$x_1 = .1977777$, $x_2 = .5230659$, $x_3 = .5013316$, $x_4 = 2.78750E\text{-}02$,
$x_5 = 1.0$, $x_6 = 0.5$

- As a result, the contribution of membership 1 of x_1(or α), membership 1 of x_2(or $\ddot{\alpha}$), membership 2 of x_3(or $\ddot{\alpha}$), membership 3 of x_4(or k), membership 1 of x_5 (or β), and membership 2 of x_6 (or δ_e) to the numerator would be 5.92943E-03.

- The contribution to the denominator is 1.43801E-03.

- Contributions from all 864 cells are evaluated to obtain 3.79087 for the numerator and 8.25118 for the denominator.

- The predicted C_L is 3.79087/8.25118 = .4594, to be compared with .4553 in the data.

· Models created with sets of data from large amplitude-oscillation tests did not predict well other sets of data at high frequencies, because these test conditions are not represented in these models.

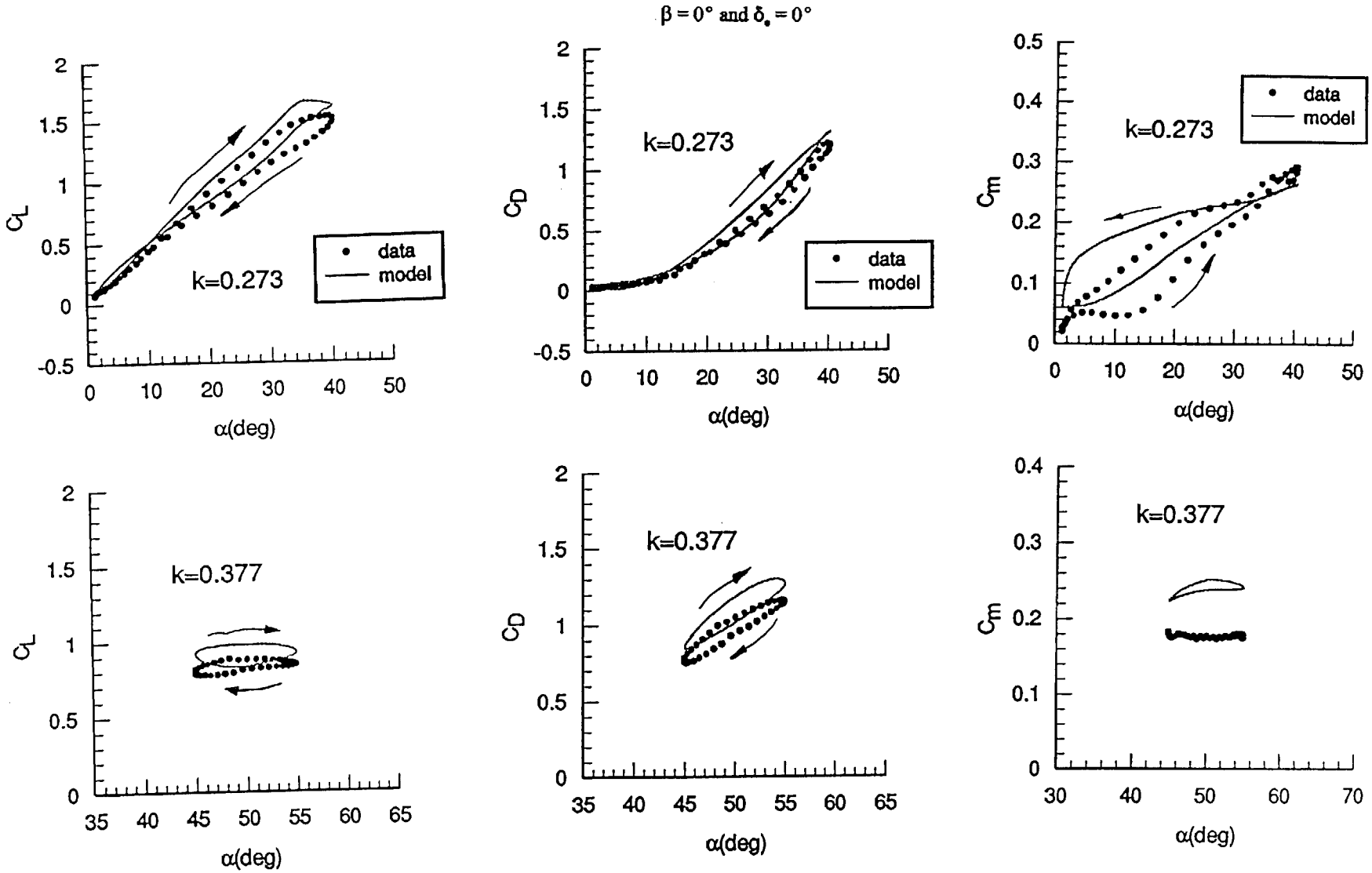

· Fuzzy logic algorithm allows these conditions to be incorporated into the models without affecting correlation with the original training data.

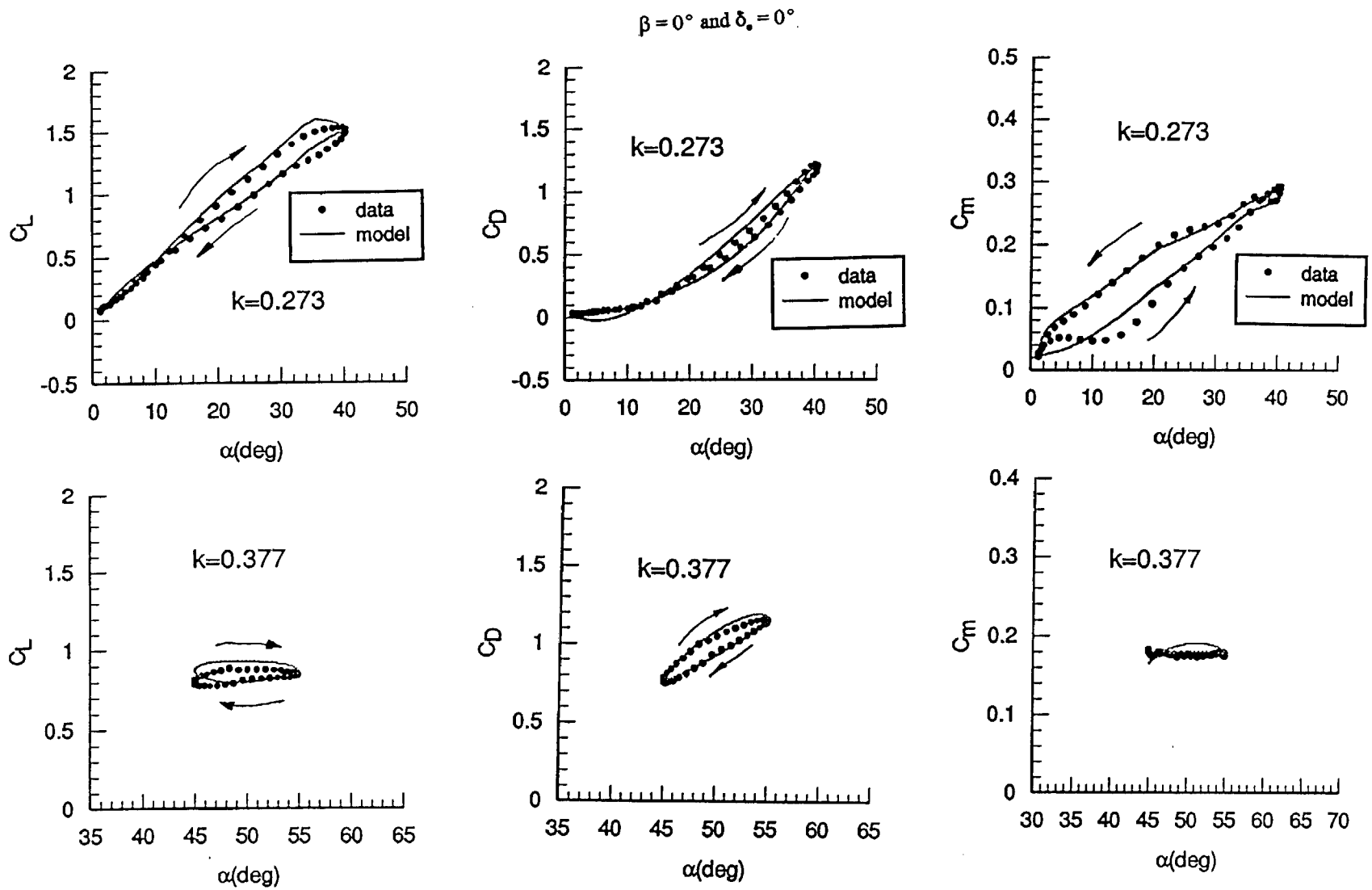

· Correlation with training data: C_L, and C_m

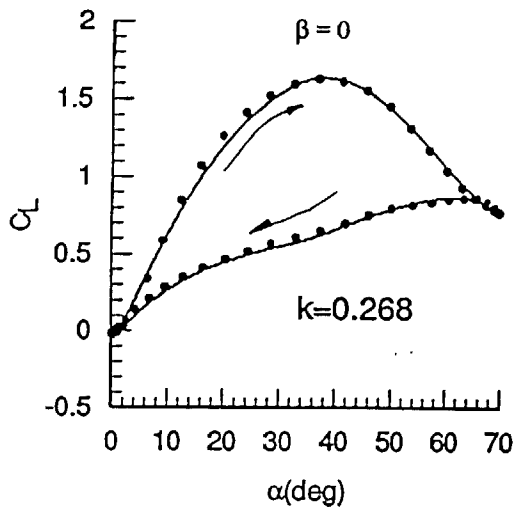

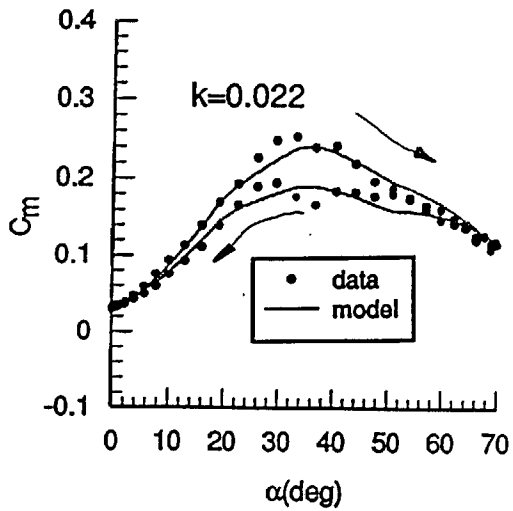

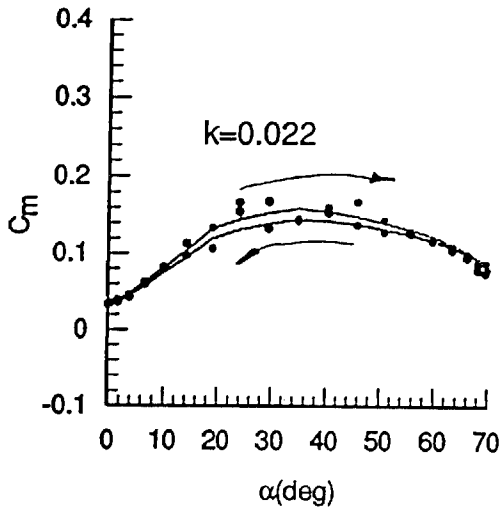

(a) β = 0

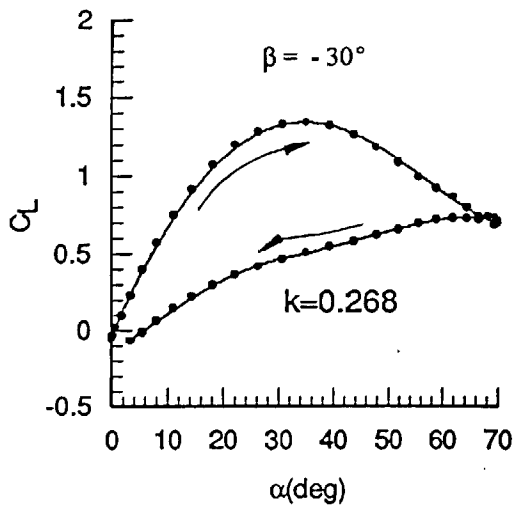

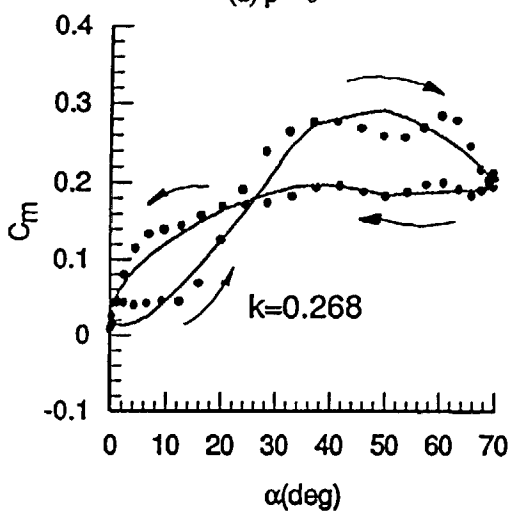

(a) β = 0

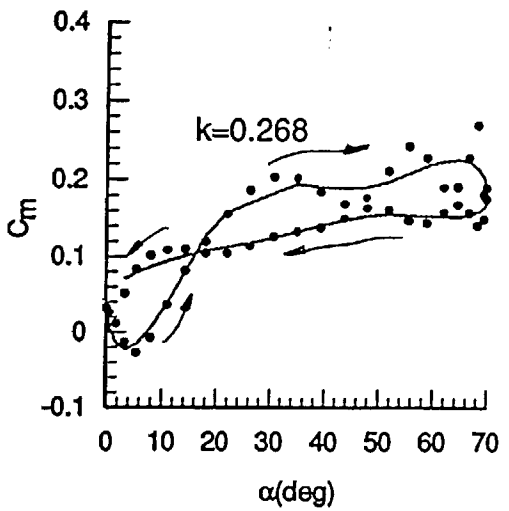

(b) β = - 30°

- Strong effect of α on directional stability
- Correlation with training data: C_n and C_ℓ

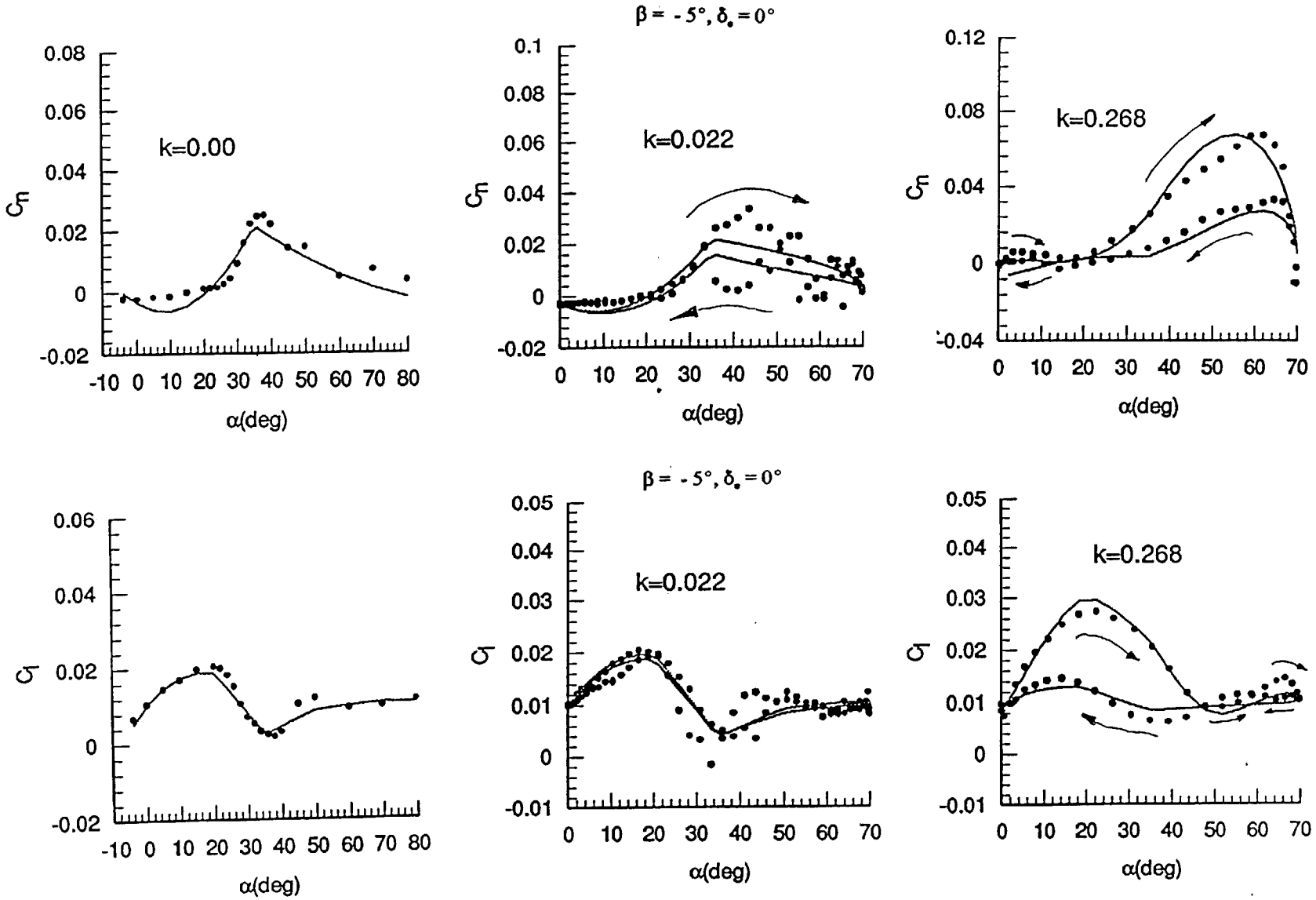

- Directional instability becomes worse by the dynamic effect
- Predicted results: C_n and C_ℓ

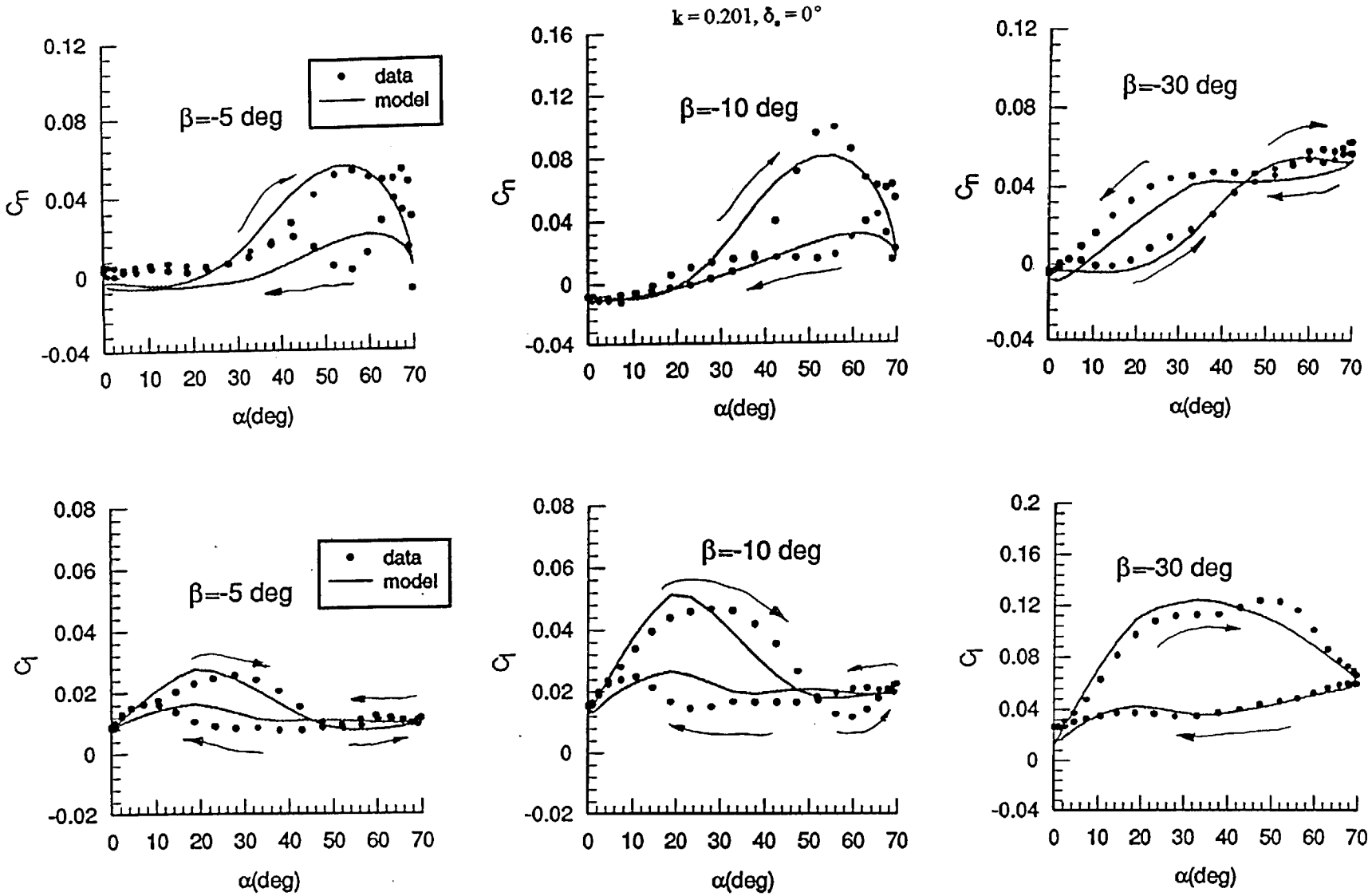

• $\ddot{\alpha}$ Effect

· The term associated with $\ddot{\alpha}$ appears as the virtual mass effect in incompressible unsteady aerodynamic theory, and could be important at high frequencies.

Predicted with $\ddot{\alpha}$

Original model

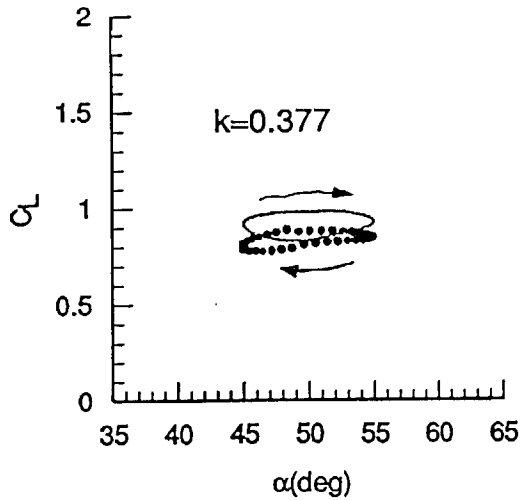

Refined model

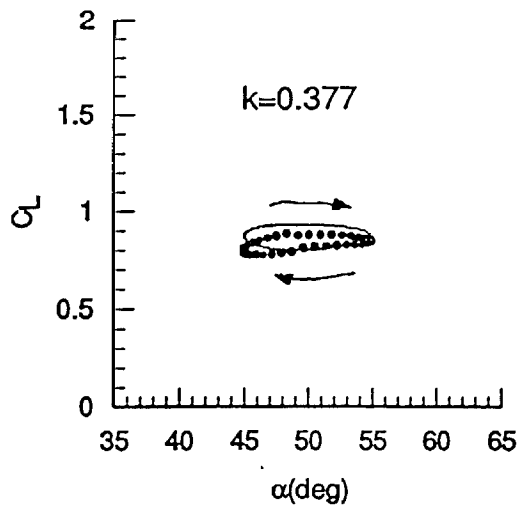

Predicted without $\ddot{\alpha}$

Original model

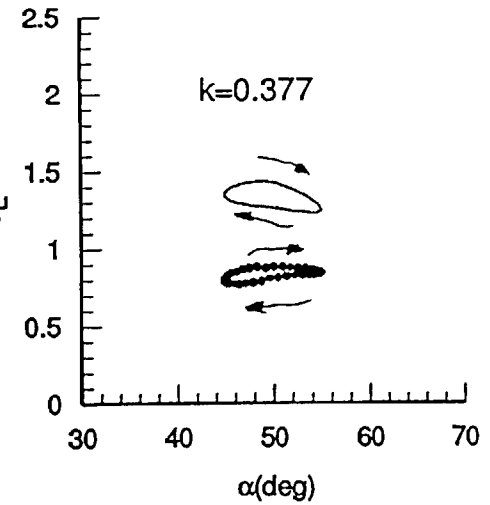

Refined model

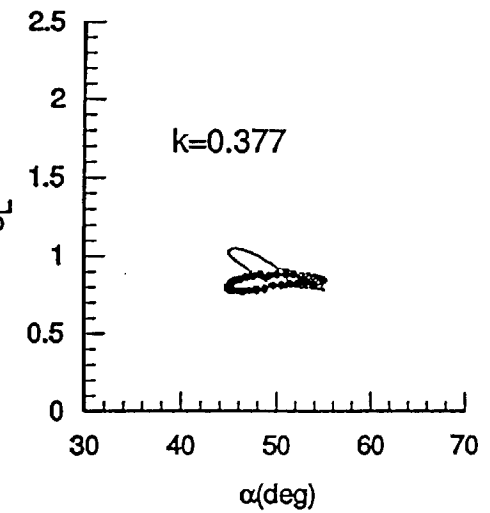

Lateral-Directional Unsteady Aerodynamics Models for an F16XL Configuration

· F16XL Lateral-Directional Aerodynamics

The unsteady aerodynamic coefficients are assumed to be functions of angle of attack α, roll angle ϕ, rate of roll angle $\dot{\phi}$, yaw angle ψ, rate of yaw angle $\dot{\psi}$, and the reduced frequency k:

$$C_{L\ ,\ D\ ,\ m,\ y,\ n,\ l} = f\ (\alpha, \phi, \dot{\phi}, k, \psi, \dot{\psi})$$

· The ranges of the motion variables are defined as:

$\alpha = 0 \sim 90°$, $\phi = -90° \sim 90°$, $\dot{\phi} = -600°/s \sim 600°/s$

$\psi = -35° \sim 35°$, $\dot{\psi} = -600°/s \sim 600°/s$,

$k = 0 \sim 0.36$

· All input variables are normalized to the domain of [0, 1]:

$$\phi_{new} = \frac{\phi - \phi_{min}}{\phi_{max} - \phi_{min}}$$

· The best model structure was determined to be:

Coefficient	α	ϕ	$\dot{\phi}$	k	ψ	$\dot{\psi}$	number of rules
C_L	5	2	2	4	3	4	960
C_D	3	2	4	3	3	4	864
C_m	5	4	2	3	4	2	960
C_y	5	4	2	2	2	2	320
C_n	6	4	2	4	2	2	768
C_ℓ	6	4	2	4	2	2	768

· For example, roll moment coefficient model with the structure: (6,4,2,4,2,2) means that the numbers of membership functions for predicting the rolling moment coefficient are 6 for α, 4 for ϕ, 2 for $\dot{\phi}$, 4 for k, 2 for ψ and 2 for $\dot{\psi}$.

• The ranges of motion variables in modeling forced oscillation test data are taken to be:

$\alpha = 0 \sim 90°$, $\phi = -35° \sim 35°$, $\dot{\phi} = -250°/s \sim 250°/s$
$\psi = -35° \sim 35°$, $\dot{\psi} = -150°/s \sim 150°/s$,
$k = 0 \sim 0.2$

• These values are increased to accommodate rotary balance data.

- Rotary balance data from a 10% model were incorporated into the aerodynamic model:

k=0. $\bar{\Omega} = \Omega b/2V = -0.4 \sim 0.4$

$$p = \bar{\Omega}(2V/b)\sin\alpha$$
$$r = \bar{\Omega}(2V/b)\cos\alpha$$

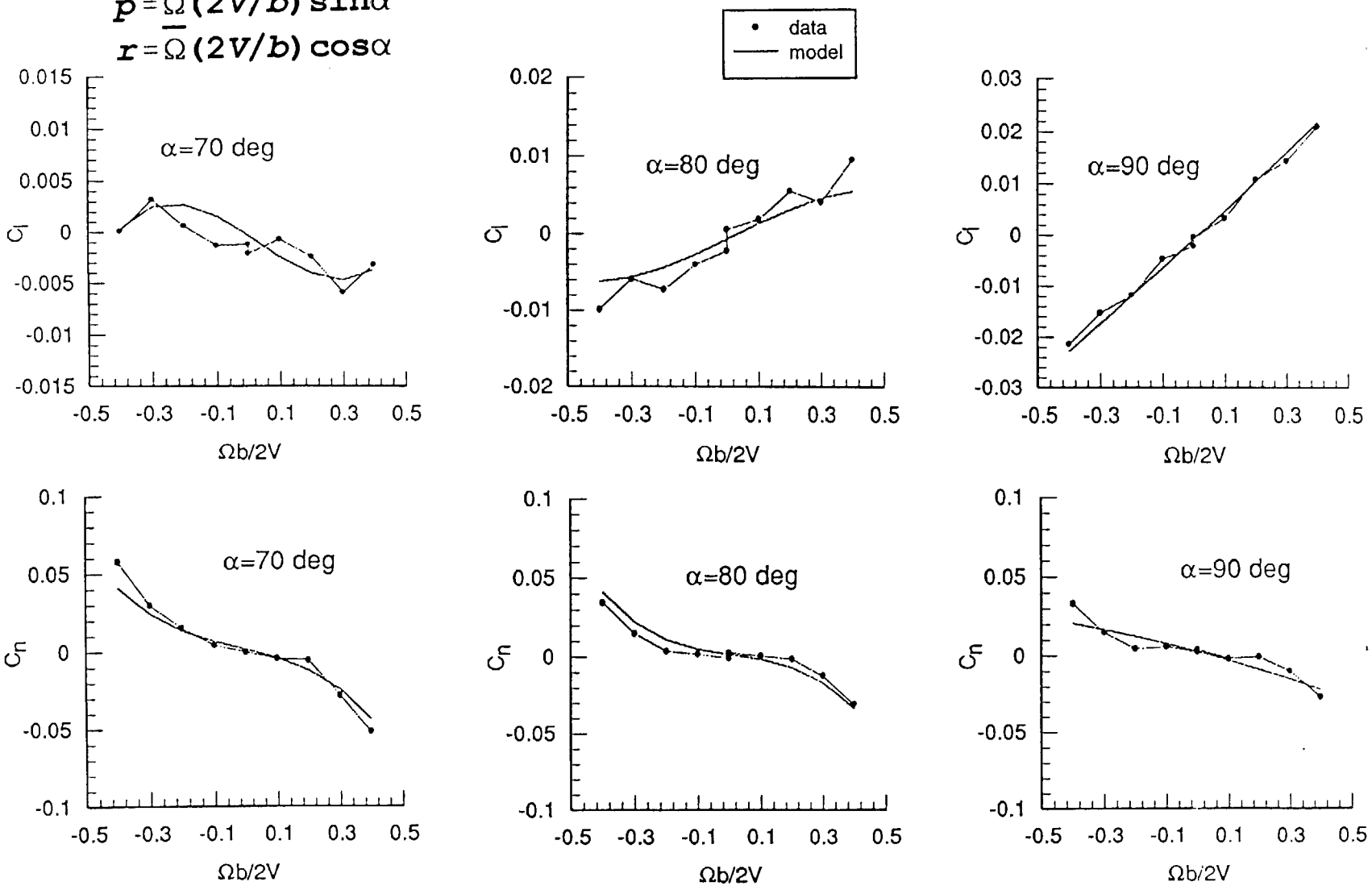

- **Model for the Rolling Moment Coefficient** - correlation coefficient = 0.948
  - C_ℓ from roll oscillation
  - A counterclockwise hysteresis loop implies positive roll damping
  - The slope of the loop indicates the magnitude of stiffness derivatives (~ C_{ℓ_β} $\sin\alpha$).

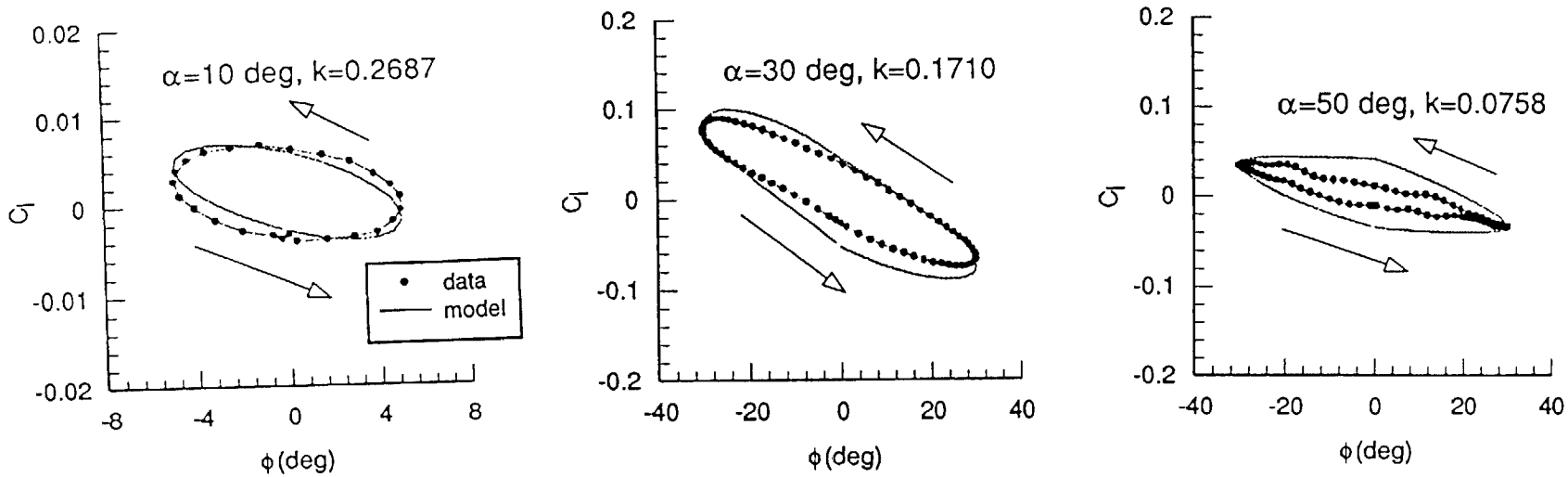

· C_ℓ from yaw oscillation

· A clockwise loop means C_{ℓ_r} is positive.

· A positive slope indicates a negative C_{ℓ_β} .

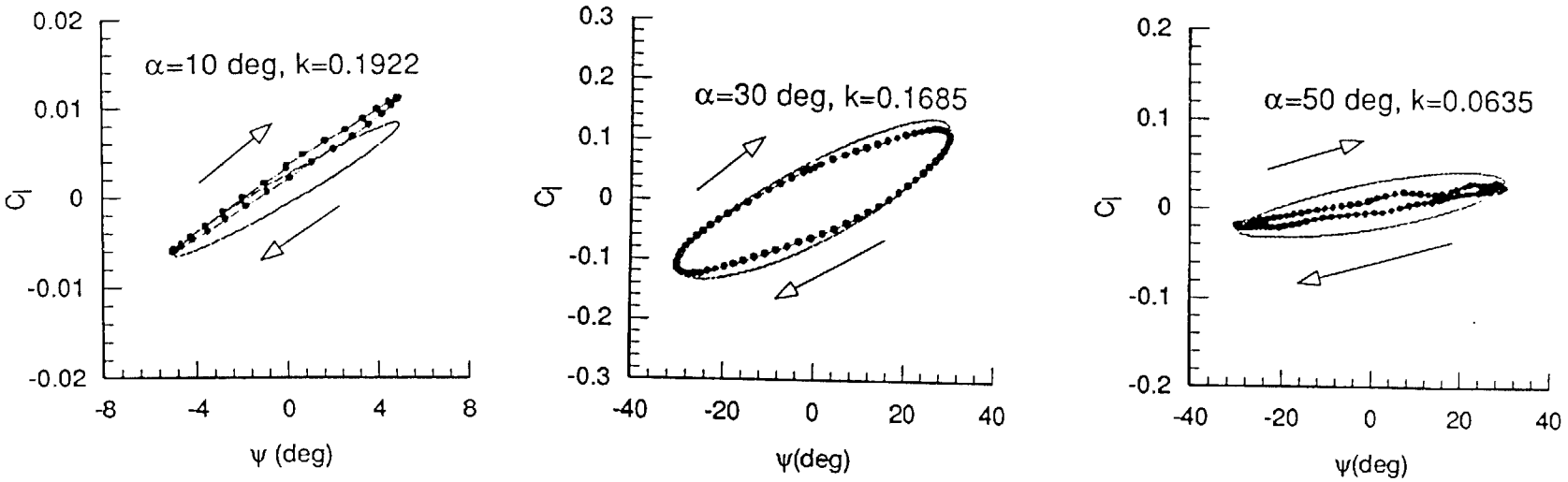

- **Model for the Yawing Moment Coefficient** - Correlation coefficient = 0.80
  - · Hysteresis loop of C_n vs ψ curves is clockwise $\Rightarrow C_{nr} > 0$.
  - · C_n measurements did not provide good correlation

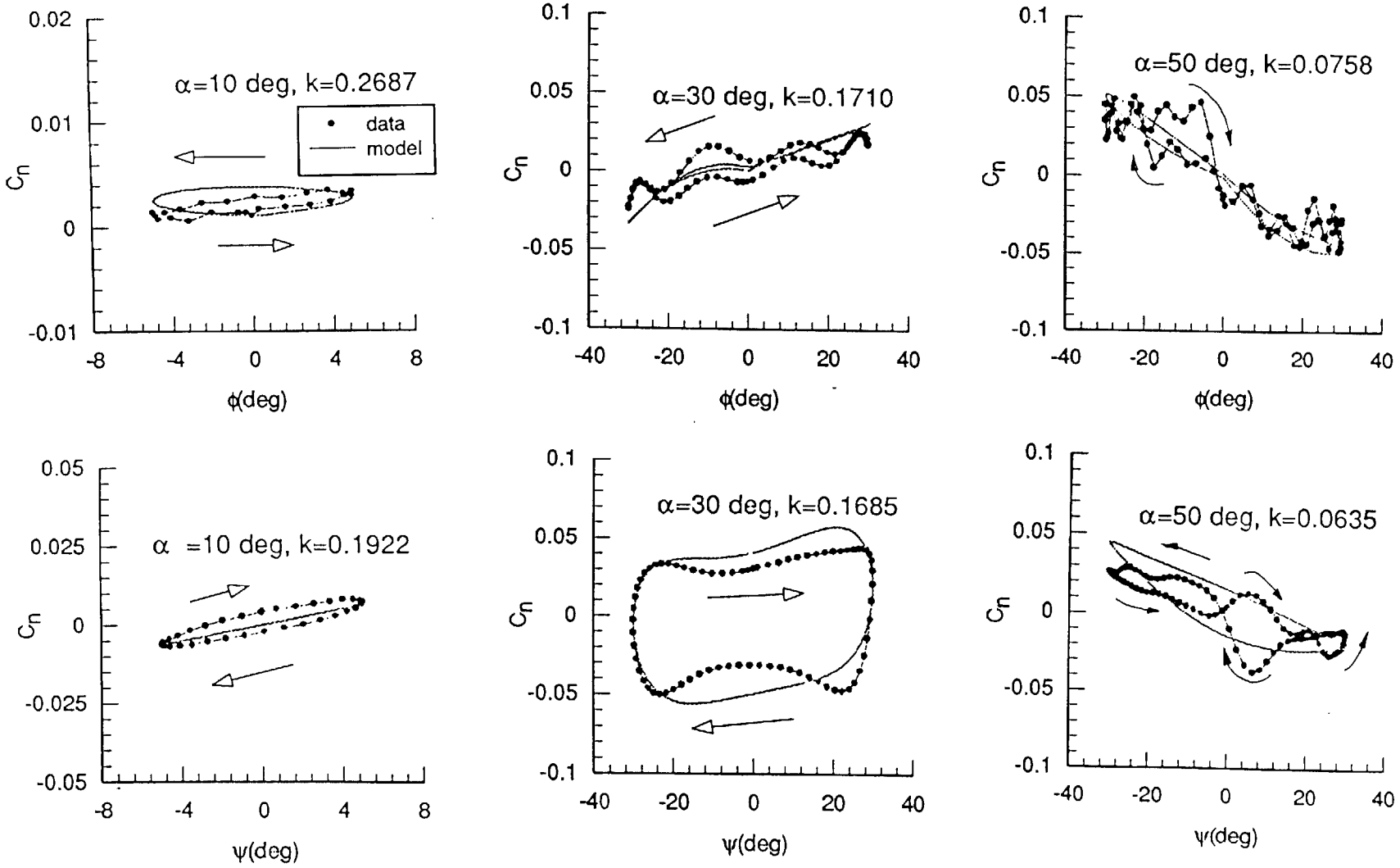

Applications

- Fuzzy-Logic Data Base for the F-16XL

  · Example: to extract forced-oscillation data with
  mean α = 20 deg. and amplitude = 20 deg.,
  at β = 0., δ_e = 0.

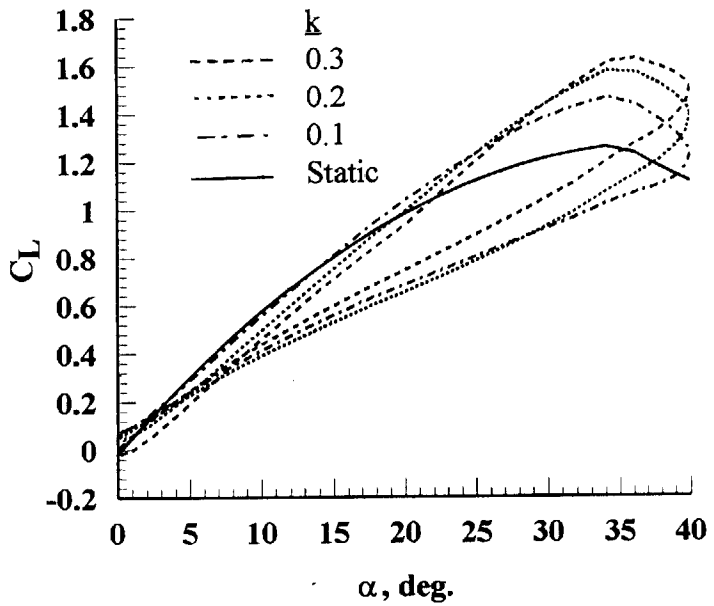

· In simulation, the unsteady aerodynamic effect is evaluated by replacing the dynamic-derivative terms in the quasi-steady formulation with the difference between the tunnel unsteady data and the tunnel static data:

$$\Delta C_n = C_n(\alpha, \phi, p, k, \psi, r) - C_n(\alpha, \phi, 0., 0., \psi, 0.)$$

· Dynamic derivatives can be evaluated with a central difference approach:

$$\Delta C_{n1} = C_n\ (\alpha, \phi, p+\Delta p, K, \psi, r) - C_n\ (\alpha, \phi, p-\Delta p, K, \psi, r)$$
$$\Delta C_{n2} = C_n\ (\alpha, \phi, p, K, \psi, r+\Delta r) - C_n\ (\alpha, \phi, p, K, \psi, r-\Delta r)$$
$$\Delta C_{\ell 1} = C_\ell\ (\alpha, \phi, p+\Delta p, K, \psi, r) - C_\ell\ (\alpha, \phi, p-\Delta p, K, \psi, r)$$
$$\Delta C_{\ell 2} = C_\ell\ (\alpha, \phi, p, K, \psi, r+\Delta r) - C_\ell\ (\alpha, \phi, p, K, \psi, r-\Delta r)$$

where $\Delta p = \Delta r = 3.0^0/s$

The dynamic derivatives at every instant are then calculated by

$$C_{np} = \Delta C_{n1} / \Delta \bar{p} \quad , \quad C_{nr} = \Delta C_{n2} / \Delta \bar{r}$$
$$C_{\ell p} = \Delta C_{\ell 1} / \Delta \bar{p} \quad , \quad C_{\ell r} = \Delta C_{\ell 2} / \Delta \bar{r}$$

·Dynamic derivatives from the quasi-steady aerodynamic model, with a rudder step input of -2 deg. at a trimmed $\alpha = 21.4$ deg.

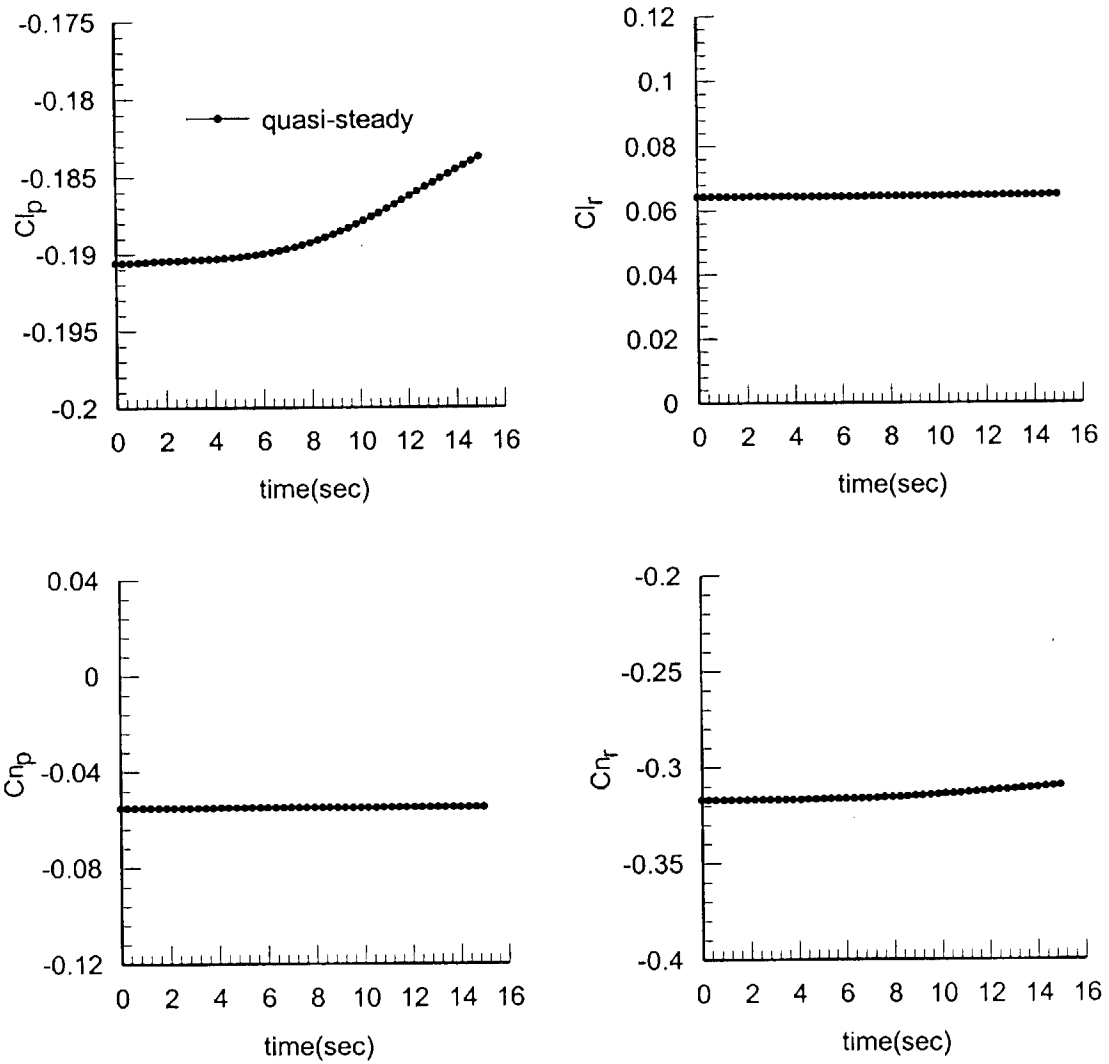

· Dynamic derivatives from the unsteady aerodynamic model, with a rudder step input of -2 deg. at a trimmed $\alpha = 21.4$ deg.

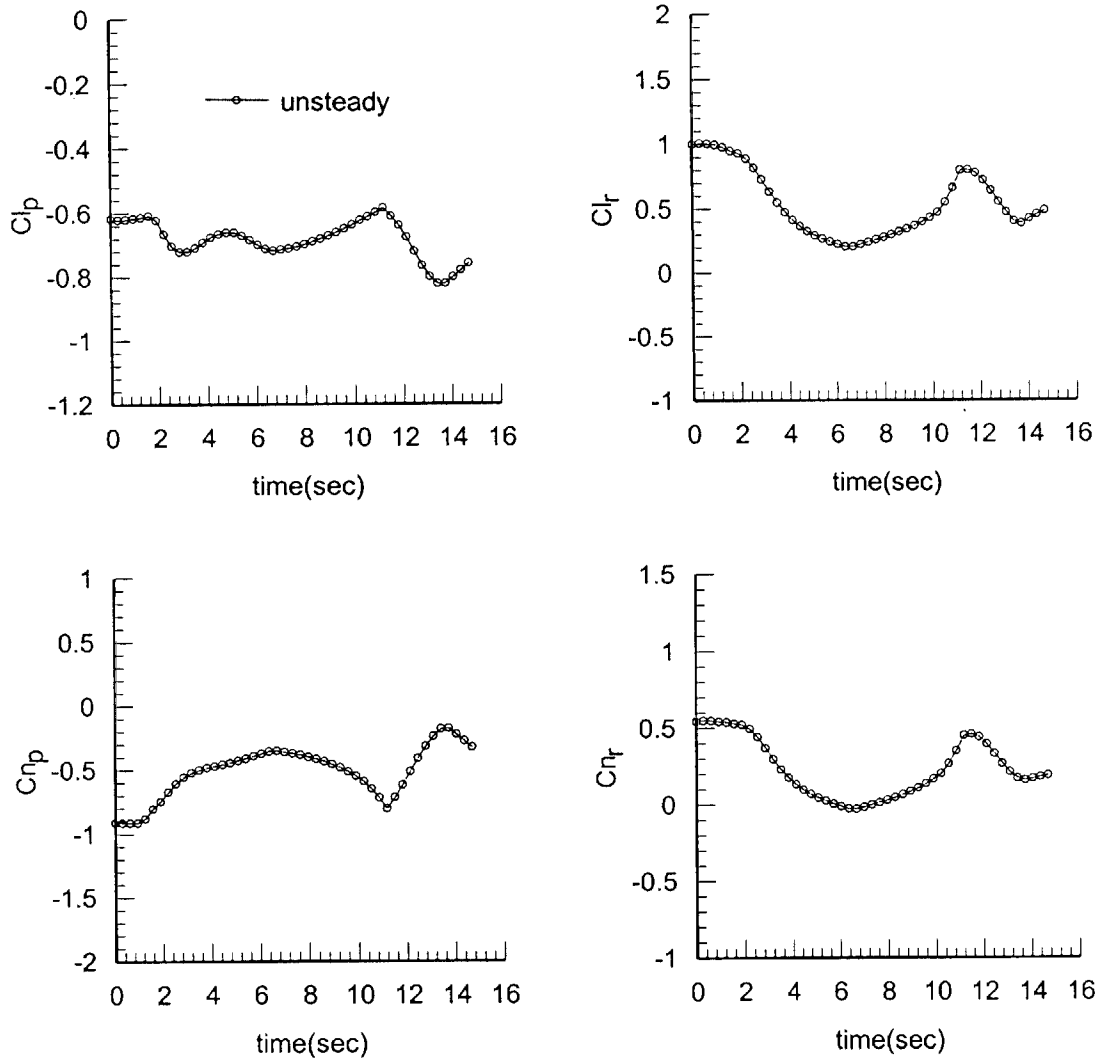

- F-18 Simulation

  - Unsteady data are adjusted to correspond to an aircraft c. g. of 0.233 $\bar{c}$.

  - The original dynamic aerodynamics (i.e. the effect of pitch damping) in the look-up tables are replaced by

    - the difference between the present unsteady and static data

  - The original pitch rate limiter and the control augmentation system are turned off.

  - The present low-speed data are assumed to be applicable at M = 0.3 and 0.5.

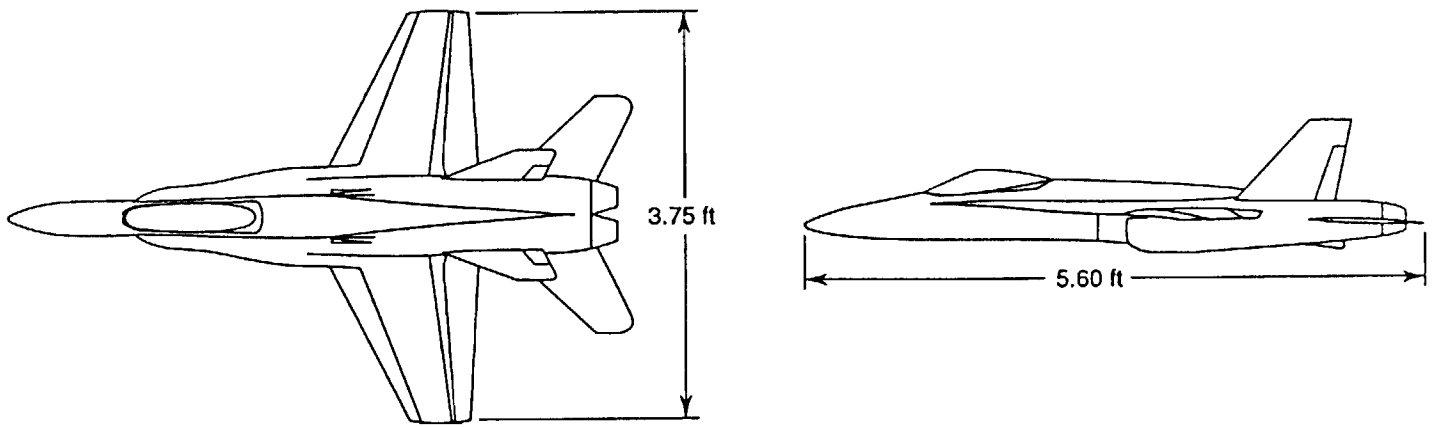

- Longitudinal Stability

  · Case 1: M=0.5, h=10,000 ft.

  ⇒ A doublet stabilator input, the stabilator being returned to - 5 deg.

  · Quasi-steady data -

  ∘ α does not reach a value at which pitch damping is negative

  ∘ The motion is stable.

  · Unsteady data -

  ∘ Lift and drag overshoot: speed decays faster.

  ∘ α and θ have divergent oscillation.

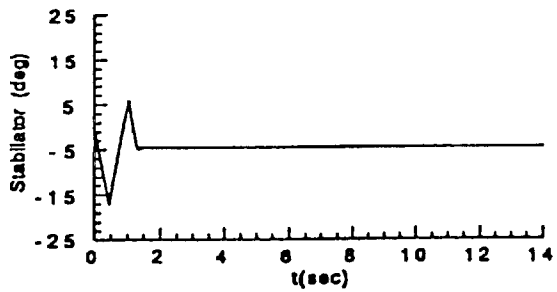

(a) Stabilator Input

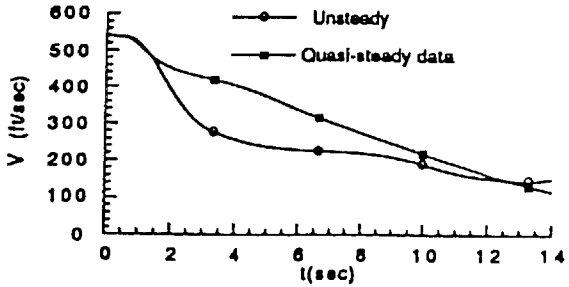

(b) Flight Speed

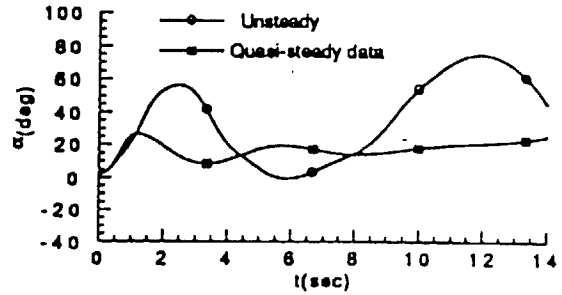

(c) Angle of Attack

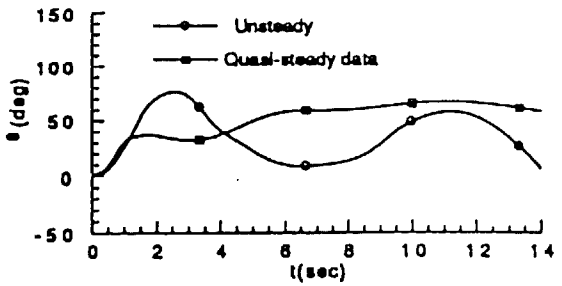

(d) Pitch Attitude

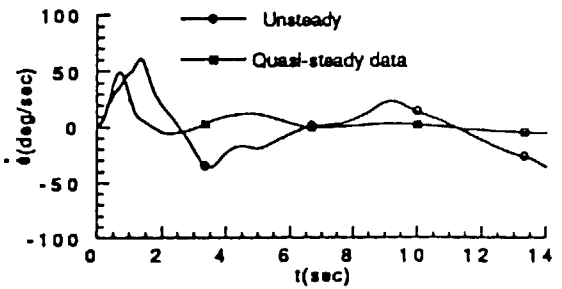

(e) Pitch Rate

- Modeling of Aircraft-Pilot Coupling
  (Ref. AIAA Paper 98-4147)

  · APC is modeled as limit-cycle oscillations.

  · To excite a limit-cycle oscillation of the short-period mode of the nonlinear aircraft system, the corresponding eigenvalue of the system matrix should have a positive real part.

    ▸ The pilot action is described as a feedback system with K_α and K_q:

  · K_α and K_q are determined by the specified eigenvalues.

  ·Predicted phase lag or time lag and frequency can be used for comparison with existing criteria.

  · PIO phenomenon is judged from the ensuing motion.

  · Pilot action is judged by the elevator angle relative to the commanded motion.

  · A nonlinear unsteady aerodynamics model for an F-18 HARV configuration ("A generalized dynamic aerodynamic coefficient model") is available.

  · Quasi-steady aerodynamic data are from SIM-2.

·The following flight conditions are taken from an analysis of equilibrium surfaces and bifurcation.

$[V, \alpha, \beta, p, q, \theta, h] = [266.7 \text{ ft/s}, 17.4°, 0, 0, 0, 9.77°, 10{,}000 \text{ ft.}]$
$[\delta_{eo}, \delta_{ao}, \delta_{ro}] = [-3.06°, 0, 0]$

$\alpha_{com} = 10$ deg., $q_{com} = 0.$

· The eigenvalues for the short-period mode based on quasi-steady aerodynamics are
$\lambda = -0.2349 \pm 1.3828i$

· Assume that
$\lambda = 0.075 \pm 1.8i$

The gains can be determined to be
$K_\alpha = 0.8305$ /deg. $K_q = -0.3514$ deg/deg/sec
These gains are maintained at all time in the simulation.

· The resulting motion is a limit-cycle oscillation:

$\phi_{ph} = -32.6°, \quad \omega = 1.514$ *rad*/sec.

$\tau_{\alpha,req} = |\phi_{ph}|/\omega = 0.38$ sec

· PIO is induced by the lag in pilot action relative to the response when the system damping is low.

· The pull-up is done when the pitch rate is increasing.

· Computed time lag $\tau_{\theta,act.} = 0.18$ sec, implying susceptibility to PIO based on the bandwidth criteria.

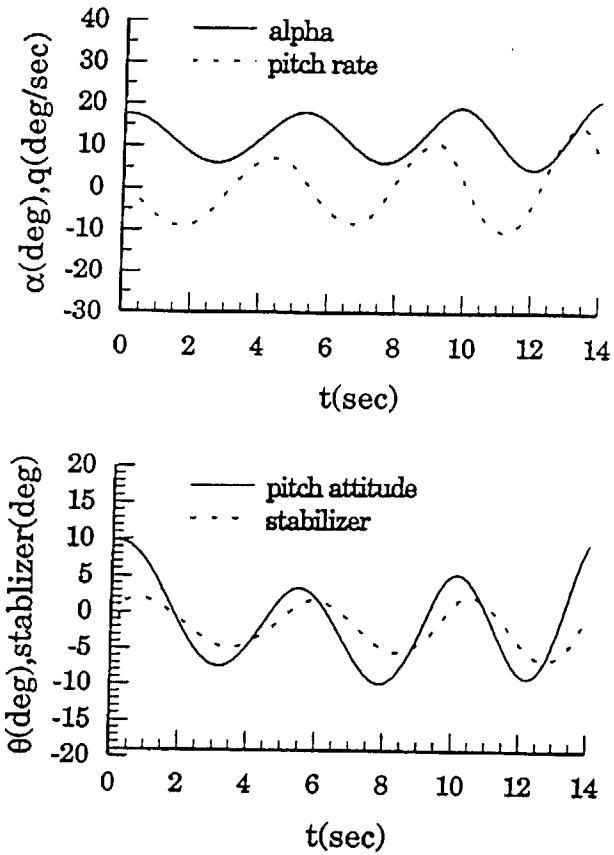

- Sensitivity Analysis

  · Increasing the real part of the specified linearized eigenvalues:

    · Time lag is increased;
    · Oscillation amplitude is increased;
    · The unsteady model requires larger time lag to develop limit-cycle oscillations and results in larger oscillation amplitudes.

  · Increasing the motion frequency:

    · Time lag is reduced;
    · Oscillation amplitude for the unsteady model is decreased;
    · Small actual time lag (< 0.14 sec) still can develop limit-cycle oscillations.

Table 1 Effect of Time Lag on Susceptibility and Severity of Pilot-Induced Oscillation for the Quasi-steady Model

ω(rad/sec)	$\tau_{\alpha.lin}$(sec)	$\tau_{\alpha.act}$(sec)	$\tau_{\theta.act}$(sec)	θ_{LCO}(deg)
1.492	0.363	0.47	0.149	.84
1.514	0.376	0.50	0.18	10.64
1.510	0.393	0.52	0.19	11.80

Table 2 Effect of Time Lag on Susceptibility and Severity of Pilot-Induced Oscillation for the Unsteady Model

ω(rad/sec)	$\tau_{\alpha.lin}$(sec)	$\tau_{\alpha.act}$(sec)	$\tau_{\theta.act}$(sec)	θ_{LCO}(deg)
1.510	0.375	0.48	0.18	11.16
1.514	0.407	0.55	0.25	15.26
1.500	0.436	0.62	0.31	15.94

Table 3 Effect of Frequency on Susceptibility and Severity of Pilot-Induced Oscillation for the Quasi-steady Model

ω(rad/sec)	$\tau_{\alpha.lin}$(sec)	$\tau_{\alpha.act}$(sec)	$\tau_{\theta.act}$(sec)	θ_{LCO}(deg)
1.215	0.560	0.81	0.34	10.18
1.514	0.376	0.50	0.18	10.64
1.750	0.281	0.35	0.09	11.04

Table 4 Effect of Frequency on Susceptibility and Severity of Pilot-Induced Oscillation for the Unsteady Model

ω(rad/sec)	$\tau_{\alpha.lin}$(sec)	$\tau_{\alpha.act}$(sec)	$\tau_{\theta.act}$(sec)	θ_{LCO}(deg)
1.269	0.561	0.85	0.45	14.30
1.514	0.407	0.55	0.25	13.22
1.721	0.317	0.40	0.10	12.48

• Maximum Gust Response in Vertical Plunging

Equation of motion:

$$MV\dot{\alpha}(t) + (1/2)\rho V^2 S C_{L_m}(t) = -L_g(t,\alpha_g,\dot{\alpha}_g)$$

Taking Fourier transform:

$$\bar{\alpha}(\omega) = \frac{-L_g(\omega)}{(i\omega)MV + (1/2)\rho V^2 S(\bar{C}_{L_m}(\omega)/\bar{\alpha}(\omega))}$$

Incremental normal acceleration:

$$\ddot{z}(t) = \mathcal{F}^{-1}[(i\omega)V\bar{\alpha}(\omega)]$$

Incremental load factor:

$$\Delta n(t) = -\ddot{z}(t)/g$$

· Results are based on Matched Filter Theory for the maximum response:

·Nonlinear unsteady aerodynamics produced 48.7% ~ 90.1% higher possible maximum incremental load factors to the von Kármán random gust than the linear unsteady aerodynamics for the F-18 HARV and the F-16XL.

· The nonlinear effect of the time rate of change in angle of attack was the main cause.

Calculated Δn_{max} from Different Aerodynamic Models

	quasi-steady	linear unsteady	nonlinear unsteady
F-18 HARV	0.267	0.417*	0.620
F-16XL	0.318	0.274	0.521

* $\Delta n_{max} = 0.387$ based on aerodynamics in plunging motion

- **General Conclusions about the Effects of Unsteady Aerodynamics**

· A statically unstable configuration is more unstable with unsteady aerodynamics

· Lateral-directional stability characteristics are significantly affected by longitudinal unsteady aerodynamics.

Recommendations

• Nonlinear stability and control analysis using simulation models with unsteady aerodynamics over the whole flight envelope and in abnormal flight conditions.

• Flight simulation in accident investigation by including unsteady aerodynamic models.

• Development of on-board dynamic loads monitoring system to provide better situational awareness to pilots.

Nonlinear unsteady aerodynamics must be included.

• Flight simulation, stability and control analysis with unsteady aerodynamic models in atmospheric turbulence (both Gaussian and non-Gaussian), thunderstorms, and icing conditions.

• Development of an engineering method to estimate nonlinear unsteady aerodynamic data at various Mach numbers.

• Development of a method to assess/correct the windtunnel wall interference in forced oscillation testing.